Journal of Geochemical Exploration 196 (2019) 219–234

Contents lists available at ScienceDirect

Journal of Geochemical Exploration

journal homepage: www.elsevier.com/locate/gexplo

Investigating the migration of pollutants at Barreiro area, Minas Gerais State, Brazil, by the ^{210}Pb chronological method

D.M. Bonotto[a,*], R. Garcia-Tenorio[b]

[a] Departamento de Petrologia e Metalogenia, Universidade Estadual Paulista (UNESP), Av. 24-A No. 1515, C.P. 178, CEP 13506-900 Rio Claro, São Paulo, Brazil
[b] Departamento de Física Aplicada II, Universidad de Sevilla, Av. Reina Mercedes No. 2, 41012 Sevilla, Spain

ARTICLE INFO

Keywords:
Open-pit mining
Niobium and phosphate exploitation
Araxá city
Barreiro area
^{210}Pb-chronological method

ABSTRACT

Barreiro area at Araxá city, Minas Gerais State, Brazil, has been subjected to intense debate because of environmental pollution related to intense mining activities developed for the phosphate and niobium exploitation. Anthropogenic inputs involving the barium release into waters occurred there by the early 1980s because of a leakage occurring at one tailings dam as the adoption of synthetic membrane for the dam waterproofing only started in 2006. This paper reports a novel (radio)chemical record obtained from the analysis of samples of waters and a 35-cm depth sediment core with the aim of focusing the major pathways for the constituents transport there, which are accompanied by information on possible modifications along the time as provided by the use of the ^{210}Pb chronological method. All waters are reducing, despite the rainwater is acid and the remaining (surface water and groundwater) are alkaline. Calcium dominates the rainwater composition, whereas Si is a relevant constituent in the surface and groundwater samples. The sediments are classified as silty sand and sand, Fe_2O_3 is the major oxide of all sediments sections, reaching a mean concentration value of 47% and it is followed by Organic Matter > BaO > SiO_2 > P_2O_5 > Al_2O_3 > TiO_2 > SO_3 > CaO > Nb_2O_5 whose mean concentration is between 2 and 15%. The Ba levels in waters and sediments from Barreiro area are high, unlike in other streams draining the Araxá municipality. Chloride exhibited a high mobility index, confirming its conservative behavior in solution, whereas the quite low value for iron corroborates that Fe oxides/hydroxides are highly sorptive materials. The CRS ^{210}Pb chronological model allowed identify BaO, Nb_2O_5, SO_3, ThO_2 and REEs (La, Ce) concentration peaks around 1973, agreeing with the significant correlations found among these parameters.

1. Introduction

The mining activities usually give rise to environmental impacts mainly due to the wastes disposal associated to the ore exploitation and processing. Acid mine drainage (AMD) generation is a typical environmental threat as can increase the metals mobility by accelerating the dissolution and leaching of minerals from the rocks and tailings piles to the environment, affecting the surface waters and groundwater quality (Filipek et al., 1987; U.S. EPA, 1994; Gray, 1996; Aksil and Koldas, 2006). Historically, mine sites are a major source of contamination to aquatic environments and countries throughout the world face severe environmental problems due to mining activities. In addition to environmental monitoring based on present-day records providing from sediments data, several studies have focused on historical changes of the environmental situation in different mine sites.

Monitoring programs are currently implemented in many mining projects, but historical data is not usually available. Luckily, lake sediments can be used to track past pollution trends, and the dating methods (e.g. ^{210}Pb method) can be used to put the sediment samples into the temporal perspective and to enable the analysis of speed and magnitude of pollution. ^{210}Pb is an intermediary member of the natural mass number (4n + 2) ^{238}U decay series that has provided a reliable dating perspective over the last 100–150 years in a wide range of environments as reported by Appleby and Oldfield (1992), Turner and Delorme (1996), among others. Some typical examples focusing the metal pollution due to the mining activities include the studies held in Sweden at the abandoned Laisvall lead mine (Widerlund et al., 2002) and in the Rakkurijoki system receiving water from the Kiruna iron mine (Widerlund et al., 2014). Additionally, it has been also investigated the migration of Hg due to its extensive use during both the colonial and post-colonial extraction of massive quantities of gold and silver in the Bolivian Andes at the headwaters of the Beni River, the

* Corresponding author.
E-mail address: dbonotto@rc.unesp.br (D.M. Bonotto).

https://doi.org/10.1016/j.gexplo.2018.10.011
Received 31 May 2018; Received in revised form 8 October 2018; Accepted 27 October 2018
Available online 04 November 2018
0375-6742/

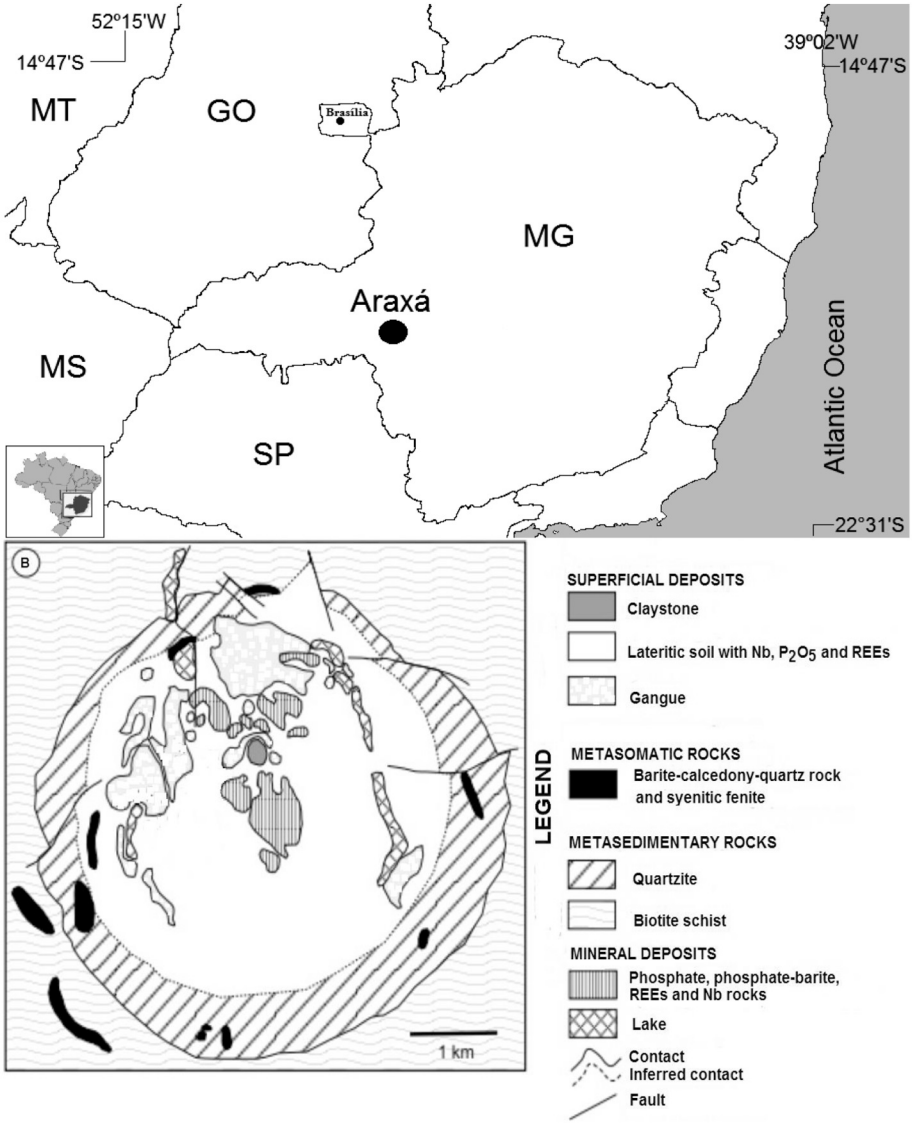

Fig. 1. (top) Location of Araxá city in Minas Gerais State, Brazil, and (B-bottom). Simplified geological map of Barreiro area modified from Traversa et al. (2001).

dispersal of Pb and Zn from an abandoned mine at Tyndrum, Scotland, the transport of heavy metals (including Pb, Cu, Zn, Cd, Cr, Co, Ni and Mn) near a copper mine at Chihu Lake in the middle Yangtze River Basin, China, and the lead pollution in Las Médulas, northwestern Spain, at the largest Roman gold mine (Maurice-Bourgoin et al., 2003; Nurlidia, 2008; Yao and Xue, 2016; Hillman et al., 2017).

The mineral sector in Brazil takes an important role in its GDP (Gross Domestic Product) as the country possesses a mineral potential equivalent or higher than that of nations like USA, Australia and Canada (Melfi et al., 2016). In Brazil, DNPM (National Department of Mineral Production) identified 10,841 "licensed mines" exploiting civil construction products/mineral waters (98.1%) and mineral commodities (1.4%) like Fe-Mn (57), Au (21), Ni-Al-Cu-Zn-Cr-Nb-Sn-Ti-W (39), and non-metallic products (phosphate-kaolin-asbestos-graphite-potassium-magnesite, 23) (Melfi et al., 2016).

Open-pit mines are widely spread in Brazil such as those located at Araxá city, Minas Gerais State (MG), which exploit niobium and phosphate and are considered of international level (Melfi et al., 2016). Araxá city is situated in southeastern Brazil at 19°35′33″S and 46°56′26″W, about 830 km distant from Rio de Janeiro (Fig. 1). The occurrence of two major springs (Dona Beja and Andrade Júnior) having different hydrochemical composition in a place known as Barreiro (about 8 km distant from Araxá city center) incentivated the tourism in the region and the construction, in 1944, of the "Grand Hotel Hydrothermal Complex" (today Grand Hotel Tauá).

Additionally, phosphate fertilizer and niobium mining activities have also occurred at Barreiro area. The phosphate research started in 1947–1948 as conducted by IPI (Industrial Research Institute), Belo Horizonte (MG), whilst the crushed ore production begun in 1960 (Viana et al., 1999). The identification of niobium in pyrochlore was in 1953, whereas its exploration initiated in 1960 (Viana et al., 1999; Lemos Jr., 2012). These mining activities have expanded since the 60's and 70's as developed by the companies *Vale Fertilizantes* (past Bunge, Arafértil) (for phosphate) and CBMM (Brazilian Company of Mining and Metallurgy) (for niobium). USGS (2018) reported a production of 20,000 tons/year of ground apatite for phosphate use in agriculture and circa 936 billion metric tons of Nb_2O_5 ore.

In Barreiro area, contaminants have been released into the environment due to the development of such mining activities, causing intense debate among population, environmental agencies, researchers, newspapermen, lawyers, companies officers, etc. (Viana et al., 1999; DA, 2008, 2009; Pinto et al., 2011; Santos et al., 2011; RBM, 2012). This paper reports a novel (hydro)geochemical record in that area with the aim of investigating the major processes affecting the constituents

transport and tracking possible modifications along the time as provided by the use of the ^{210}Pb chronological method.

2. Study area

Araxá city is in an average elevation of 973 m above sea level and its climate type according to Nimer (1972) classification is tropical sub-hot and semi-wet (i.e. mean temperature of the colder month of 15 °C–18 °C at least in one month, and 4–5 dry months). The mean annual temperature in the region is 20.6 °C with maximum around 32 °C and minimum around 4 °C (Beato et al., 2000). The average total annual rainfall is ~156 cm, and the total annual evapotranspiration is ~97 cm, with the rainy season occurring between October and April (Beato et al., 2000).

The Alto Paranaíba Igneous Province (APIP) is one of the world's most voluminous mafic potassic province composed of a relatively diverse suite of ultrapotassic-potassic, ultramafic-mafic, silica-undersaturated lavas and hypabyssal intrusions with very high concentrations of incompatible trace elements and strong enrichment in light REEs relatively to the heavy ones (Gibson et al., 1995; Gomes and Comin-Chiaramonti, 2005). It includes Barreiro area, also reported in the literature as Araxá complex, which comprises the renowned Araxá carbonatite circular intrusion (diameter ~4.5 km) and is located in a fractured zone tending to a major NW direction (Traversa et al., 2001) (Fig. 1). Barreiro area comprises a complex network of concentric and radial carbonatite dykes of variable size and millimetric to centimetric veins intruding either alkaline or country rocks. Additional lithologies include mica-rich rocks, phoscorites and lamprophyres (Traversa et al., 2001).

The weathering layer resulting from the alkaline-carbonatite rocks alteration is very thick, sometimes higher than 200 m. Enrichment of P_2O_5, Nb_2O_5, TiO_2, BaO and REE_2O_3 occurs in the weathered material, whose distribution in the intrusion area is irregular, reflecting the complex lithology of the alkaline association (Braga and Born, 1988). Several changes occurring in pyrochlore [$A_2B_2X_7$; A (Na, Ca, Ba, K, U) and B (Nb, Ta, Ti)] provide abundant barium-pyrochlore at Barreiro area, where Ba and Nb dominate the A and B positions, respectively (Braga and Born, 1988). The weathering processes promoted the pyrochlore enrichment in the central portion of the circular structure that originated one of the largest world niobium deposit (Issa Filho et al., 1984).

The weathering mantle also contains a large phosphate reserve situated at the northwestern portion of the complex, comprising an area of about 2.5 km^2 and including the presence of an apatite-shaped material (Braga and Born, 1988). The following materials exempt of apatite (despite the P_2O_5 presence) embrace the weathered cover: a dark reddish layer composed by hydrated iron oxides, clay minerals, and disperse/concentrated limonite blocks; a matrix resulting from the extreme weathering of the original constituents. A zone containing apatite occurs below the superficial weathered cover, which is dark brown colored and characterized by the presence of significant CaO levels and P_2O_5 content above 20% (Braga and Born, 1988).

Different pyrochlore generations are responsible by the uranium presence at Barreiro area. U can occur widely disseminated in the mineral matrix as a trace constituent (100 ppm U_3O_8) or may characterize an uraniferous pyrochlore (2% U_3O_8) (Castro and Souza, 1970). The secondary U-minerals autunite and uranocircite have been identified in some restrict areas, in which they are filling rock fractures chiefly containing apatite and barite. The U_3O_8 concentration range is 150–200 ppm in the phosphate deposit area (Castro and Souza, 1970). In addition, U also occurs associated to the REEs-enriched carbonatite that formed the closed ellipsoidal structure at the central-northern portion of Barreiro area (Castro and Souza, 1970).

Grand Hotel lake dominates the Barreiro area landscape that is highlighted by the presence of the springs Dona Beja and Andrade Júnior (Fig. 2). Recharging rainwater sustains two major aquifer systems in the region, whose discharge happens when the water table intercepts the terrain surface due to the topographic constraints. The first is a shallower, granular, and free aquifer, locally semi-confined by clayey levels of the weathered layer. The second is a deeper, fractured, free to semi-confined aquifer, mainly occurring in rocks around the carbonatite complex and outcropping in an area where the rock has not suffered significant alteration (FUNTEC, 1984; Beato et al., 2000). The surface waters drainage at Barreiro area comprises a western and eastern zone, in which occur Baritina stream (and tributaries) together with the BCM dam and mine dyke (Fig. 2) that drain the mining and waste disposal sites of the phosphate mine. Baritina stream also receives waters providing from the niobium mining, flowing into the Grand Hotel direction.

2.1. Niobium exploitation at Barreiro area

The activities developed by CBMM at Araxá city for the Nb exploitation are relevant for this study. Most of the niobium has been transformed into Fe-Nb for use in steel industries, despite parts of the production plant have been adapted for including the increasing demand on REEs (CBMM, 2015). Its production cycle involves several steps for obtaining the pyrochlore concentrate as crushing, milling, magnetic separation, mud removal and flotation (Fig. 3). The Nb_2O_5 concentration is about 60% in the pyrochlore concentrate, whereas the wastes consist mainly of magnetite (15%), mud (15%) and flotation material (70%) (Gomes, 2006; Lemos Jr., 2012).

The final pyrochlore concentrate is transferred to another unit at CBMM for calcination and leaching (Fig. 3), which involves treatment with 5% HCl for reducing the impurities (P, S, Pb) content (do Rio, 1999). Sulfuric acid solubilizes barium in this pyrochlore concentrate, whilst the slags deposit receives the barium sulfate formed (Fig. 3). The tailings dam (B4) takes on the discharges of the by-products comprising the supernatant solution neutralized with lime and barium chloride (do Rio, 1999; Beato et al., 2000). The metallurgical plant gets the leaching concentrate for performing reduction chemical reactions (Fig. 3).

The dam for wastes disposal (B5) supplies recirculation water for use in the pyrochlore concentration unit and acid leaching plant (Fig. 3). Gomes (2006) reported the increase of the water reservoir in the tailings dam B5 during the rainy season, implying on the need of pumping the water into a treatment station for later release to a watercourse crossing the area (Fig. 3).

3. Experimental

3.1. Sampling

The fieldwork was done between June and October 2009, corresponding to the dry period and beginning of the wet season. Samples of surface water (20 L) and sediment core (35 cm deep) were collected from Grand Hotel lake at Barreiro area, Araxá city (Fig. 2). The coring site selection was due to its favorable topographic condition for receiving surface waters and effluents providing from the two major mining areas (phosphate fertilizer and niobium) at Barreiro area. Additional groundwater samples (20 L) were taken from Dona Beja and Andrade Júnior springs discharging nearby, as well from rainfall recovered by a bulk collector (dry and wet deposition) as described by Cresswell and Bonotto (2008) and installed close to the unit dedicated for processing phosphate fertilizer. The Wildco Model 77263 hand core sampler permitted the sediment core collection as reported by Bonotto and Lima (2006). In situ readings for temperature, pH, conductivity, and potential redox (Eh) of the water samples followed the analytical protocol reported by Bonotto (2016). The water samples were stored in polyethylene flasks, whilst the sediment core was kept under refrigeration at about 2 °C and put vertically in a properly designed metallic apparatus. Under these conditions occurred their transportation to LABIDRO-Isotopes and Hydrochemistry Laboratory of IGCE/ UNESP/

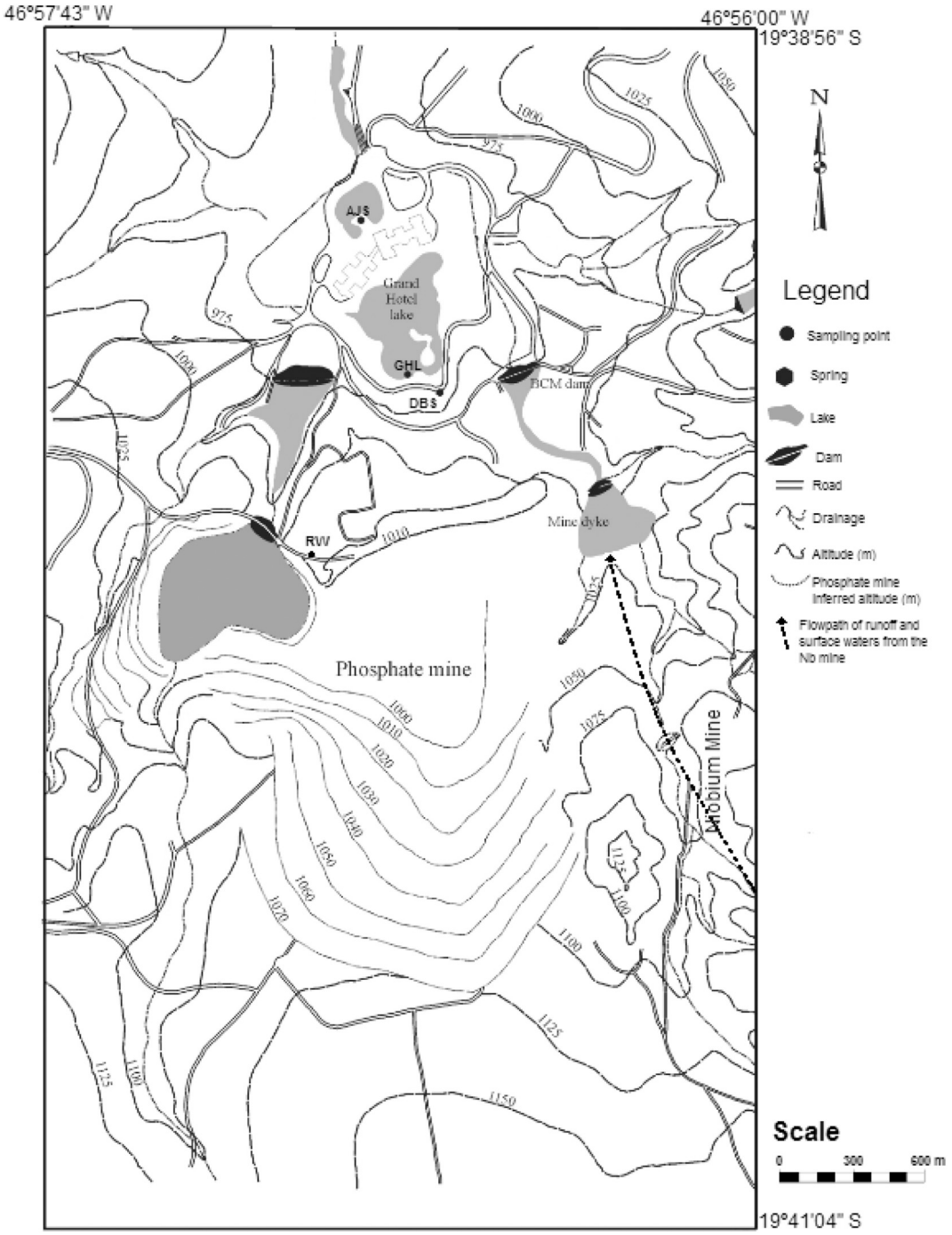

Fig. 2. Location of the sampling points at Barreiro area, Araxá city, Minas Gerais State, Brazil. Table 1 shows each sample identification code. Base map modified from FUNTEC (1984).

Rio Claro for the chemical analyzes.

3.2. Chemical composition of the waters and sediments

In the laboratory, the water samples were divided in different aliquots after filtration with 0.45 μm Millipore membrane, comprising the material retained to the Total Suspended Solids (TSS) phase. The sediment core was extruded with a polyethylene embolus and cut into 5-cm segments with a porcelain spatula (Bonotto and Lima, 2006), whereas TSS was subjected to acid digestion (HNO_3) for chemical analysis of the particulate matter. Evaporation to dryness, titration with 0.02 N H_2SO_4, atomic absorption spectrometry (AAS), colorimetry, ion-selective electrode, and inductively coupled plasma atomic emission spectrometry (ICP-AES) allowed generate the hydrochemical data as detailed by Hach (1992), Bonotto and Silveira (2003), van de Wiel (2003), and Rice et al. (2012).

The spectrophotometry (Hach, 1992) permitted characterize the organic matter (OM) in each sediments slice. The moisture (M) was determined after its drying at 60 °C during ~24 h for avoiding the OM and volatile compounds losses, according to the equation M (%) = 100(TM – DM / TM), where TM and DM are the total mass and dry mass, respectively, both in g. The porosity (ϕ) estimate was done using the formula $\phi = (TM - DM) / \{TM + DM\ [(\rho_1 / \rho_2) - 1)]\}$, where ρ_1 is the water density (1 g/cm^3) and ρ_2 is the sediments (quartz)

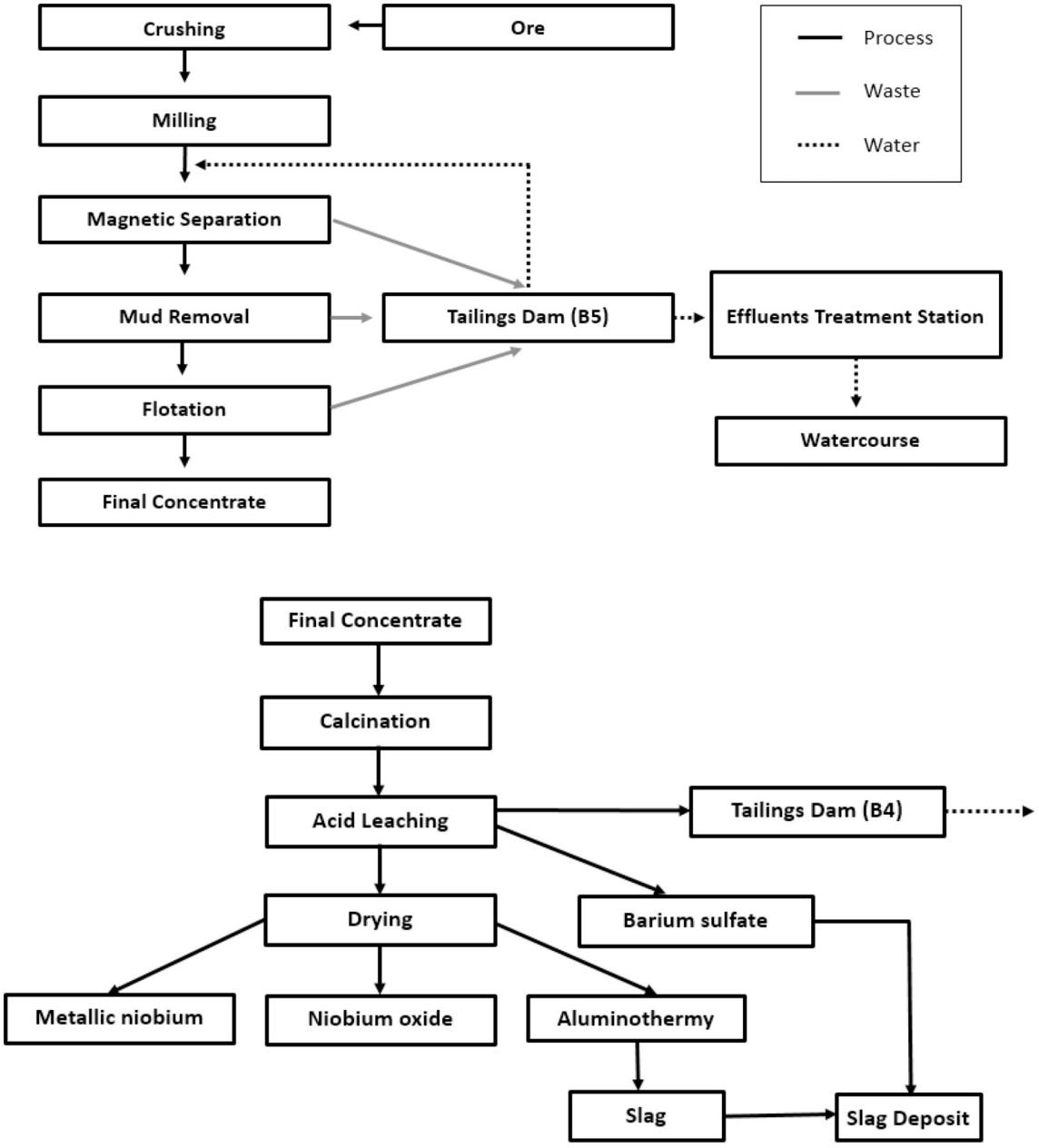

Fig. 3. Sketch simplified diagram showing the major steps involved in the niobium production by CBMM, Araxá city, Minas Gerais State, Brazil. Modified from do Rio (1999) and Gomes (2006).

density (2.65 g/cm^3) (Argollo, 2001). The mass depth (MD, in g/cm^2) in this paper corresponded to the division of the DM by the corer area, whilst the Munsell (1975) chart allowed classify the sediments color.

Bonotto and Lima (2006) described the procedures adopted for the separation of each sediments segment into aliquots for grain size, leaching experiments, X-ray diffraction, X-ray fluorescence, and radiochemical analyses. The Udden (1898) scale (in mm) and Wentworth (1922) classification of the sediments particles size were coded as GRA = granule (> 2.0 mm), VGS = very gross sand (2.0–1.0 mm), GRS = gross sand (1.0–0.5 mm), AVS = average sand (0.5–0.25 mm), FIS = fine sand (0.25–0.125 mm), VFS = very fine sand (0.125–0.063 mm), GSI = gross silt (0.063–0.037 mm), and ASI = average silt (< 0.037 mm).

The high-end wavelength dispersion X-ray fluorescence spectrometer S8 TIGER from Bruker Co. installed at LARIN-Ionizing Radiation Laboratory of UNESPetro (Geosciences Center Applied to Petroleum), IGCE/UNESP/Rio Claro, provided the major and trace constituents data in the sediments (Roveratti and Bonotto, 2017). Leaching experiments of the sediments sections (2.5 g inserted into 250 mL glass bottles) took place in the laboratory under the following conditions: room temperature (~20 °C); leaching time = 24 h; leachant = 150 mL distilled water equilibrated with the atmosphere (CO_2 partial pressure $\sim 10^{-3.5}$ atm and pH = 5.65). The solutions were periodically agitated along the experiment to ensure that the leachant concentration remained uniform throughout the solution and that surface leach occurred at a constant rate. Barium, chloride, sulfate, phosphate, and nitrate analysis in the leachates was done by Hach DR2000 spectrophotometer at appropriate wavelengths (Hach, 1992).

3.3. Radiochemical analysis of the sediments and waters

The analytical protocol reported by Bonotto and Vergotti (2015) allowed measuring ^{210}Pb in the lake sediments after quantifying its granddaughter ^{210}Po, whereas a relatively similar procedure applied to

~10 L of each water sample permitted to measure the dissolved ^{210}Po activity concentration as detailed by Bonotto et al. (2009). The dissolved U concentration (in μg/L) in the surface and groundwater samples was determined after applying the radiochemical procedure reported by Bonotto (2010).

Another digestion of different aliquots (0.6–1.6 g) with *aqua regia* (1:3 HNO_3-HCl) allowed obtain information about the parent-supported (in-situ produced) ^{210}Pb, $^{210}Pb_s$, in all sections of the sediment core. The analytical steps as described by Bonotto (2010) consisted on the ^{232}U spike (4.4 dpm) addition, Fe^{3+} extraction with isopropyl ether, use of anionic exchange resin, U-electrodeposition in stainless steel disks and adoption of alpha spectrometry for acquiring the U activity concentration data, named [U]. The condition of radioactive equilibrium between ^{238}U and ^{226}Ra was checked using the γ-rays spectrometry through a 3 × 3″ NaI(Tl) scintillation detector. This technique permitted to perform readings of the eU (equivalent uranium = ^{226}Ra) in the same sections of the sediment core. The eU range was 4.0–28.8 μg/g (average = 12.6 μg/g) and denoted slight deviation of the equilibrium condition in some sections of the sediment core. However, the [U] and eU records implied in a difference of only 3% in the linear sedimentation rate. The better sensitivity of the alpha relative to the gamma spectrometric readings was the reason for adopting the [U] instead of eU data in this paper.

The parent-supported (in-situ produced) ^{210}Pb, $^{210}Pb_s$, was calculated from the equation $^{210}Pb_s = 0.16 \times [U]$, which takes into account the expected Rn atoms fraction formed in the solid phase that will contribute to the $^{210}Pb_s$ generation. The ^{222}Rn emanation coefficient (E) from the rock matrices and soils/sediments is highly dependant of the specific surface area (particles size) and moisture, among other parameters (e.g. Appleby and Oldfield, 1992; Bonotto and Andrews, 1997, 1999; etc.). Wanty et al. (1992) pointed out that the E values are generally < 0.5. For instance, they are 0.01–0.34 (average = 0.1) in minerals like thorianite and carbonite or 0.01–0.18 (average = 0.07) in minerals from granitic rocks (Appleby and Oldfield, 1992), 0.1–0.2 in soils from the Mendip Hills area, England (Bonotto and Andrews, 1999), average = 0.2 in different types of rocks and soils (UNSCEAR, 2000), 0.00083–0.07 for unheated, pulverized samples from three different mineral groups (Krupp et al., 2017), and 0.03–0.17 in different soil types (Saad et al., 2018).

The factor 0.16 adopted for calculating $^{210}Pb_s$ arises of ^{222}Rn losses estimation yielding E values of 0.36–0.84 from the laboratory timescale experiments reported by Bonotto and Caprioglio (2002) for different samples of sedimentary rocks crushed to grain sizes compatible to the sediment core in this study. Wanty et al. (1992) and UNSCEAR (2000) reported high E values like 0.7 and above in different situations, thus, confirming the feasibility of such accentuated Rn exhalation. The choice of the factor 0.16 was due to its successful use in previous studies focusing the ^{210}Pb chronological method (e.g. Bonotto and Lima, 2006; Sabaris and Bonotto, 2010; Nery and Bonotto, 2011; Matamet and Bonotto, 2013, 2018; Bonotto and Garcia-Tenorio, 2014; Bonotto and Vergotti, 2015). The same factor also permitted Fontana et al. (2014) to track the eutrophication history of a tropical water supply reservoir, i.e. Guarapiranga Reservoir that is the second most important public water supply in São Paulo State, Brazil. The historical record in that site was compatible with the year of the reservoir construction (1909) and a historically documented event in the basin also served as a good chronological marker (Fontana et al., 2014).

The excess ^{210}Pb activity, $^{210}Pb_{xs}$, corresponded to the difference between total and supported activities: $^{210}Pb_{xs} = {}^{210}Pb_T - {}^{210}Pb_s$. The mean analytical uncertainty (1σ standard deviation, 5% significance level) of the radiometric data was 12% ($^{210}Pb_s$) and 6% ($^{210}Pb_T$) as calculated from the errors propagation theory (Young, 1962). The CF:CS (Constant Flux: Constant Sedimentation) and CRS (Constant Rate of ^{210}Pb Supply) models have been applied to the $^{210}Pb_{xs}$ dataset as reported elsewhere (e.g. Krishnaswami et al., 1971; Appleby and Oldfield, 1978; El-Daoushy, 1988; Baskaran and Naidu, 1995; San Miguel et al., 2001; Kotarba et al., 2002; Bonotto and Garcia-Tenorio, 2014).

The CF:CS model assumes a constant $^{210}Pb_{xs}$ flux incorporated into the sediments and also a constant sedimentation rate, producing an exponential ^{210}Pb activity decrease according to the sediments column depth (San Miguel et al., 2001). Under such conditions, plotting ln $^{210}Pb_{xs}$ against the mass depth (MD, in g/cm^2) results in a linear ^{210}Pb profile whose slope is $-\lambda_{210}/f$ (λ_{210} = ^{210}Pb radioactive decay constant, 0.0311 yr^{-1}; f = sedimentation rate, gcm^{-2} yr^{-1}) (Baskaran and Naidu, 1995).

The CRS model assumes that for a certain aquatic system the total annual unsupported ^{210}Pb fluxes delivered to, and maintained by, a depositional sequence should be constant during the past two centuries (Krishnaswami et al., 1971; Appleby and Oldfield, 1978; Robbins, 1978). The age t of a certain level at which the unsupported ^{210}Pb inventory integrated over the whole profile (A_0, total inventory; in dpm/g) has declined to A_x (in dpm/g) satisfies the equation (El-Daoushy, 1988; Kotarba et al., 2002):

$$A_x = A_0 . e^{-\lambda_{210} t} \text{ or } t = (1/\lambda_{210}) . \ln (A_0/A_x) \quad (1)$$

where: A_x corresponds to the inventory of $^{210}Pb_{xs}$ from the layer at depth x (formed t years ago) to the bottom of the sediment core, or to the last layer $^{210}Pb_{xs}$ is detected in. The sedimentation rate r_x at the depth x according to the CRS model may be calculated by the following formula (Appleby and Oldfield, 1978; Kotarba et al., 2002):

$$r_x = MD . \lambda_{210} . (A_x/C_x) \quad (2)$$

where: C_x (in dpm/g) is the unsupported ^{210}Pb activity at depth x.

4. Results and discussion

4.1. Major trends from the chemical data

Table 1 reports the analytical data obtained for the water samples. According to temperature, the Brazilian guideline for mineral waters (Vieira, 2004) indicates that they are cold (≤25 °C, samples GHL and DBS) and hypothermal (25–33 °C, sample AJS). This implies on different groundwater circulation depths in the aquifer systems related to the DBS and AJS waters. The parameters pH and Eh represent, respectively, the protons and electrons activities in the environment (Krauskopf and Bird, 1995; Brownlow, 1996). They indicate that all waters are reducing, RW is acid and the remaining waters are alkaline (Fig. 4). The electrical conductivity (and TDS) was highest in groundwater AJS and lowest in RW (Table 1). The Schoeller (1962) diagram (Fig. 4) shows that Na justifies such trends due to its dominant preponderance in AJS relative to RW. This diagram also highlights the calcium dominance in RW relative to other waters (Fig. 4). Plotting the analytical data in a Piper (1944) diagram (Fig. 4) shows the calcium dominance of RW, (bi)carbonate facies of the DBS and AJS groundwaters and tendency of the mixed character for dissolved anions in GHL and RW samples. The Schoeller (1962) diagram (Fig. 4) also points out that Si is a relevant constituent in the surface and groundwater samples as previously identified by Bonotto (2016) in other Brazilian geological contexts. The fluoride concentration of AJS groundwater is above the WHO (2011) guideline reference value (1.5 mg/L) like verified in some other spas groundwaters in southern Brazil (Bonotto, 2016).

Tables 2–4 report the results obtained for all sediments sections analyzed. The dominant sediments color is dark brown, gross sand (1.0–0.5 mm) prevails at 10–15 cm depth, gross silt (63–37 μm) preponderates at 20–25 cm depth, whereas fine sand (250–125 μm) overwhelms in all other depths. According to the Shepard (1954) nomenclature, the sediments are silty sand (20–25 cm depth) and sand (all other depths). The sediments porosity ranged from 2.6 to 19.7%, and the OM concentration between 9 and 21%. The vertical profile of porosity shows an abrupt change in the layers 15–20 cm and 20–25 cm depth, where the moisture is higher, as a consequence of the formula

Table 1
Results of the analyses of water samples collected at Barreiro area, Araxá city, Minas Gerais State, Brazil.

Sample identification (code)	Grand Hotel lake (GHL)	Grand Hotel lake (GHL-SS)[a]	Rainwater (RW)	Rainwater (RW-SS)[a]	Dona Beja spring (DBS)	Andrade Júnior spring (AJS)
Temperature (°C)	22.0	–	26.0	–	22.1	29.0
pH	8.48	–	5.92	–	8.56	10.72
Eh (mV)	−64	–	−59	–	−52	−103
Conductivity (μS/cm)	880	–	50	–	270	7140
TDS[b] (mg/L)	123	–	30	–	70	2898
TSS[c] (mg/L)	–	5.3	–	17	–	–
SiO_2 (mg/L)	15.3	< 0.10	1.6	< 0.10	23.4	20.3
HCO_3^- (mg/L)	52	–	11	–	112	52
CO_3^{2-} (mg/L)	0	–	0	–	0	2160
OH^- (mg/L)	0	–	0	–	0	0
Cl^- (mg/L)	23.6	–	2.1	–	2.1	48
SO_4^{2-} (mg/L)	7	–	1	–	3	189
NO_3^- (mg/L)	1.8	–	3.3	–	5.3	2.3
F^- (mg/L)	0.08	–	0.26	–	0.29	9
PO_4^{3-} (mg/L)	0.01	< 0.01	0.37	< 0.01	0.29	1.36
Na^+ (mg/L)	12	0.90	1.7	0.40	2.1	1510
K^+ (mg/L)	4.8	0.60	1.8	0.40	8.8	14.9
Ca^{2+} (mg/L)	2.64	1.63	6.66	0.35	0.17	0.42
Mg^{2+} (mg/L)	0.11	0.16	0.32	0.06	0.32	0.11
Sr (mg/L)	2.47	0.02	0.01	0.002	–	–
Ba (mg/L)	1.31	0.03	0.009	0.007	1	1
Cd (mg/L)	< 0.10	< 0.10	< 0.10	< 0.10	–	–
Fe (μg/L)	0.16	96	1.40	165	60	40
Al (μg/L)	5.79	181	17.06	372	–	–
Ni (μg/L)	0.49	5	0.54	< 0.10	–	–
Cu (μg/L)	0.79	60	1.42	410	–	–
Zn (μg/L)	0.35	38	5.34	149	–	–
Mn (μg/L)	< 0.10	< 0.10	1.56	< 0.10	–	–
Cr (μg/L)	0.28	9	< 0.10	10	–	–
Co (μg/L)	0.28	< 0.10	< 0.10	< 0.10	–	–
Pb (μg/L)	0.56	< 0.10	< 0.10	44	–	–
U (μg/L)	0.69	–	–	–	0.16	0.06
^{210}Po (mBq/L)	5.36	–	10.16	–	9.96	8.30

[a] Suspended solids; nm = not measured.
[b] TDS = total dissolved solids.

adopted for estimating porosity that is directly dependant of the moisture values. Similar changes also happened in other sediment core in the region, for instance, at Sal stream (layers 5–10 cm and 20–25 cm depth) and at Feio stream (layers 0–5 cm, 15–20 cm and 35–40 cm depth). Fe_2O_3 is the major oxide of all sediments sections, reaching a mean concentration value of 47% (Table 3). It is followed by OM > BaO > SiO_2 > P_2O_5 > Al_2O_3 > TiO_2 > SO_3 > CaO > Nb_2O_5 whose mean concentration is between 2 and 15%. The high Ba and Nb levels in the sediments is evident, surpassing those of the most common oxides Na_2O, K_2O and MgO occurring in the sediments profiles (e.g. Bonotto and Garcia-Tenorio, 2014). Barite (45%), goethite (21%), and hematite (20%) are the major mineral phases identified by X-ray diffraction analysis, in contrast with quartz whose abundance is only 3%.

Unlike the sediments profiles reported by Bonotto and Garcia-Tenorio (2014) and sampled at four riverine systems occurring in the Brazilian states of São Paulo (Corumbataí River, Atibaia River, and Ribeirão dos Bagres basins) and Amapá (Amazon River mouth), OM did not correlate significantly with the constituents reported in Table 3. On the other hand, several direct and inverse significant correlations exist among the major constituents, U, Th, REEs, $^{210}Pb_T$, etc., as shown in Table 5. A detailed evaluation of all relationships is beyond the scope of this paper, but some of them possibly highlight that the sediments composition reflects the presence of distinct associations formed during the weathering processes affecting the source minerals in the Barreiro area. For instance, BaO and Nb_2O_5 correlated with Fe_2O_3 (r = 0.83 and 0.75, respectively), SO_3 (r = 0.95 and 0.86, respectively), CeO_2 (r = 0.68 and 0.87, respectively), La_2O_3 (r = 0.66 and 0.85, respectively), and ThO_2 (r = 0.95 and 0.98, respectively) (Table 5). Such relationships could be related with the sources materials consisting of pyrochlore possessing pronounced Ba and Nb concentration, iron oxides, sulphide minerals and REE-phosphate monazite enriched in ThO_2 (Traversa et al., 2001). Quartz, silicates (olivines, clinopyroxenes, amphiboles, micas) and apatite possessing large amounts of P_2O_5 and CaO in the Barreiro area as pointed out by Traversa et al. (2001) could be the source materials justifying the following relationships with SiO_2: K_2O (r = 0.89), CaO (r = 0.82), P_2O_5 (r = 0.78), $^{210}Pb_T$ (r = 0.90) (Table 5). All these significant correlations imply on other reported in Table 5, as well those involving the sections depth of the sediment core as plotted in Fig. 5.

4.2. Elements mobility from chemical data and leaching experiments

CSWRCB (1995), NOAA (1999), CCME (2001), Simpson et al. (2005), among other, have proposed sediments quality guidelines elsewhere. In Brazil, the CONAMA Resolution No. 344 from 7th May 2004 ruled the standards for the sediments quality in the country based on MacDonald (1993), Long et al. (1995) and CCME (2001). CCME (1995) established guidelines for different chemicals based on the threshold effect level (TEL) and the probable effect level (PEL). They

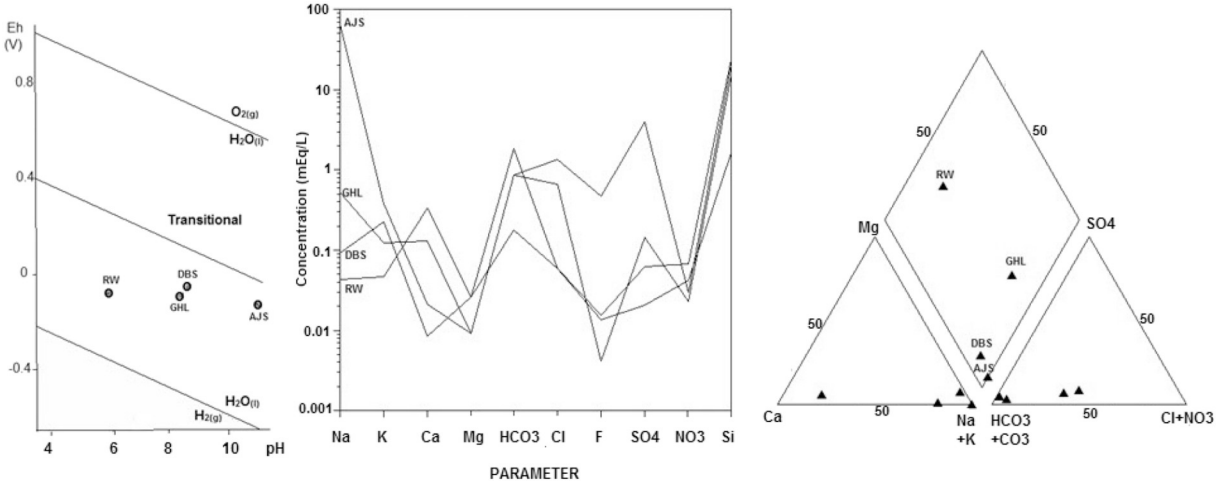

Fig. 4. Data of the waters in this research plotted in (left) Eh-pH diagram as reported by Krauskopf and Bird (1995), (middle) Schoeller (1962) diagram, and (right) Piper (1944) diagram.

Table 2
(top) Main characteristics of the sediment core sampled at Barreiro area, Araxá city, Minas Gerais State, Brazil, and (bottom) Results for barium, chloride, phosphate, sulfate and nitrate of the sediments leaching with distilled water equilibrated with the atmosphere.

Depth range (cm)	Color[a]	Total mass, TM (g)	Dry mass, DM (g)	MD[b] (g/cm^2)	Weight (%)								Moisture, M (%)	Porosity, ϕ (%)
					GRA[c]	VGS[c]	GRS[c]	AVS[c]	FIS[c]	VFS[c]	GSI[c]	ASI[c]		
0–5	DBR	83.44	82.62	4.21	0	9.37	15.16	21.10	30.15	12.80	7.36	4.05	0.98	2.56
5–10	DBR	95.09	93.98	8.99	0	13.03	21.44	21.55	22.06	13.00	5.59	3.32	1.17	3.03
10–15	DBR	115.65	112.80	14.74	0	15.60	20.50	18.88	18.37	12.43	9.81	4.40	2.46	6.27
15–20	DBR	26.88	24.60	15.99	0	5.17	14.06	20.24	22.73	18.34	11.83	7.63	8.48	19.72
20–25	BLK	81.00	74.46	19.78	0	2.69	8.78	15.52	23.26	19.47	25.00	5.28	8.07	18.88
25–30	RBR	135.93	134.54	26.64	0	1.58	10.76	21.47	28.74	19.97	16.22	1.26	1.02	2.66
30–35	RBR	105.21	101.61	31.81	0	3.12	9.76	15.23	30.51	28.58	9.26	3.54	3.42	8.58

Depth range	Amount leached (mg/L)				
(cm)	Barium	Chloride	Phosphate	Sulfate	Nitrate
0–5	15.7	14.7	0.80	3.5	3.9
5–10	16.8	15.6	0.71	3.5	4.0
10–15	15.7	13.8	0.76	2.3	2.8
15–20	18.0	16.5	2.47	0.6	3.5
20–25	16.2	14.1	0.94	0.6	3.2
25–30	15.1	15.0	2.80	1.2	2.6
30–35	15.7	14.1	0.96	0.6	2.1

[a] Munsell (1975) classification: DBR = dark brown (7.5YR 3/3); BLK = black (7.5YR 25/1); RBR = reddish brown (5YR 4/4).
[b] MD = mass depth.

represent the upper limit of the range of sediment chemical concentrations for avoiding hazards to aquatic organisms (TEL) and the lower limit of the range of chemical concentrations that is usually or always associated with adverse biological effects (PEL).

The mean value obtained for Cr, Zn, Cu and Pb from data reported in Table 3 is 157, 1020, 336 and 464 μg/g, respectively, which exceeds the PEL for freshwater corresponding to 90, 315, 197 and 91.3 μg/g, respectively (CCME, 2001). The average value for As (11 μg/g) is between TEL (5.9 μg/g) and PEL (17 μg/g) (CCME, 2001). Such enhanced levels of heavy metals in the analyzed sediments sections should be

Table 3
Chemical analyses of the sediment core sampled at Barreiro area, Araxá city, Minas Gerais State, Brazil.

Depth range (cm)							
Constituent (%)	0–5	5–10	10–15	15–20	20–25	25–30	30–35
OM[a]	15.04	21.48	11.76	13.48	19.80	15.44	9.06
SiO_2	14.05	10.00	7.52	9.74	3.28	3.75	2.85
Al_2O_3	5.53	5.90	6.97	8.41	4.77	5.07	3.93
Fe_2O_3	42.90	45.46	46.77	41.31	49.16	52.51	52.15
TiO_2	5.08	5.01	5.68	8.36	4.43	4.28	4.64
Na_2O	0.11	0.08	0.11	< 0.01	0.13	0.09	0.16
K_2O	0.19	0.17	0.16	0.12	0.02	0.06	< 0.01
CaO	3.94	3.84	3.71	2.17	1.64	1.52	1.49
MgO	0.38	0.28	0.30	0.23	0.29	0.29	0.27
MnO	0.53	0.73	0.95	0.24	0.26	0.39	0.28
P_2O_5	7.52	7.49	8.58	9.26	4.70	4.62	3.97
BaO	11.58	12.58	11.70	11.73	17.43	15.40	17.61
Nb_2O_5	1.46	1.52	1.37	1.56	3.23	2.65	2.51
SO_3	3.80	3.81	2.75	2.30	6.17	5.37	6.86
SrO	0.61	0.66	0.72	0.99	0.72	0.71	0.60
ZrO_2	0.16	0.17	0.20	0.35	0.18	0.15	0.14
Cr_2O_3	0.04	0.03	0.04	0.10	0.04	0.04	0.03
ZnO	0.10	0.11	0.12	0.17	0.15	0.13	0.11
CuO	0.04	0.04	0.03	0.07	< 0.01	0.03	0.04
NiO	0.02	0.02	0.04	0.03	0.02	0.02	< 0.01
PbO	0.04	0.04	0.04	0.06	0.06	0.06	0.05
Cl	0.02	0.02	0.02	0.03	0.01	< 0.01	< 0.01
As_2O_3	0.0047	0.0042	0.0049	0.0006	0.0012	0.0020	0.0023
ThO_2	0.10	0.11	0.10	0.12	0.19	0.17	0.17
La_2O_3	0.48	0.49	0.52	0.66	0.83	0.72	0.59
CeO_2	0.93	1.07	1.13	1.08	1.69	1.48	1.11
Nd_2O_3	0.36	0.32	0.42	0.52	0.51	0.47	0.35
Y_2O_3	0.03	0.04	0.05	0.08	0.04	0.03	0.03
Gd_2O_3	0.0014	< 0.001	0.0055	0.09	0.02	< 0.001	< 0.001

[a] OM = organic matter.

Table 4
Radiochemical data of the sediment core sampled at Barreiro area, Araxá city, Minas Gerais State, Brazil.

Depth range (cm)	MD ($g{\cdot}cm^{-2}$)	[U][a] ($dpm{\cdot}g^{-1}$)	^{210}Po[a] ($dpm{\cdot}g^{-1}$)	Total ^{210}Pb activity, $^{210}Pb_T$ ($dpm{\cdot}g^{-1}$)	In situ ^{210}Pb activity[b], $^{210}Pb_s$ ($dpm{\cdot}g^{-1}$)	Excess ^{210}Pb activity[c], $^{210}Pb_{xs}$ ($dpm{\cdot}g^{-1}$)	ln ($^{210}Pb_{xs}$) ($dpm{\cdot}g^{-1}$)	Deposition time[d] (years) CRS model	Deposition year CRS model	Sedimentation rate[e] ($g{\cdot}cm^{-2}{\cdot}yr^{-1}$) CRS model
0–5	4.21	7.91 ± 0.7	39.16 ± 1.9	39.16	1.26	37.89	3.63	0	2009	0.53
5–10	8.99	6.13 ± 0.5	22.76 ± 1.8	22.76	0.98	21.78	3.08	9 ± 1	1999–2001	1.47
10–15	14.74	10.60 ± 2.9	20.59 ± 1.1	20.59	1.70	18.89	2.94	16 ± 1	1992–1994	2.26
15–20	15.99	22.90 ± 1.4	27.26 ± 1.4	27.26	3.66	23.60	3.16	23 ± 1	1985–1987	1.56
20–25	19.78	12.64 ± 1.8	17.64 ± 1.0	17.64	2.02	15.62	2.75	36 ± 2	1971–1975	1.99
25–30	26.64	8.54 ± 0.8	18.74 ± 1.4	18.74	1.37	17.37	2.85	47 ± 4	1958–1966	1.66
30–35	31.81	5.67 ± 0.6	18.42 ± 1.1	18.42	0.91	17.51	2.86	70 ± 4	1935–1943	0.99
									Mean	1.49

[a] Analytical uncertainty corresponding to 1σ standard deviation.
[b] $^{210}Pb_s = 0.16$ [U].
[c] $^{210}Pb_{xs} = {}^{210}Pb_T - {}^{210}Pb_s$.
[d] Eq. (1) in the text.

associated with the mineralization present in the central portion of the circular structure at Barreiro area. They are at least equivalent to values reported in other polluted sites like the estuary of the River Acushnel at New Bedford Harbor, Massachusetts, USA (Cr, Na, Cu, and Pb; Stoffers et al., 1977), Yenshui River at southern Taiwan (Cr; Chang et al., 1998), Persian Gulf (Cr; Karbassi et al., 2005), lakes of the Gniezno Lake District and Rybnik dam reservoir at Poland (Cr, Zn and Cu; Baran and Tarnawski, 2015; Bojakowska and Krasuska, 2014), or Yellow River at China (Cr; Shang et al., 2015).

The Ba and Nb concentrations are high at Barreiro area (Table 3). In the case of barium, its toxicity has been generally attributed to the ions Ba^{2+} that are readily absorbed from the gastrointestinal tract and lung as the intestinal mucosa of mammals is highly permeable to them, contributing to their rapid movement into the blood (DiBello et al., 1991). Despite CCME (1995) did not establish guideline reference values for Ba in the sediments, CCME (2013) reported them in the Soil Quality Guidelines for the protection of environmental and human health, which corresponded to 750 μg/g for agricultural land use, 500 μg/g for residential/parkland land use, and 2000 μg/g for commercial/industrial land use. The mean value obtained for Ba from data reported in Table 3 is circa 167 times higher than the guideline reference value proposed by CCME (2013) for soil use in agriculture and about 306 times higher than the maximum value of 409 μg/g reported by Bojakowska and Krasuska (2014) in polluted sediments of lakes near Konin, Poland. Studies focusing the effects of the high levels of Ba, Nb, Cr, Zn, Cu and Pb on the ecology of the lake sudied here have not been done yet, constituting Ba a very important target for bioassays investigations similar to those conducted by Baran and Tarnawski (2015), among other.

In order to investigate the mobility of elements and how heavy metals and other constituents may become bound in soils and sediments would be desirable to compare the content in interstitial water with that of the solid phase as this comparison might give insight of the processes involved and of the influence of the pollution events. However, such approach is more resources consuming than other also helpful as a rough indicative, for instance, adoption of different geochemical indexes, proper leaching procedures and reagents (e.g. Langmuir, 1978; Tessier et al., 1979; Krauskopf and Bird, 1995; Faure, 1998; Komárek and Zeman, 2004; Huong et al., 2010; Barbieri, 2016).

The leaching experiments in this paper provided data on the water-soluble fraction that is the first step in the selective sequential extraction (SSE) (Tessier et al., 1979; Huong et al., 2010). The constituents data in sediments elutriates (water-soluble fraction of the sediments) are helpful for indicating sediments contamination, allowing comparison with the water quality standards (U.S. FWS, 2007). The mean value obtained for Ba, Cl^-, PO_4^{3-}, SO_4^{2-} and NO_3^- in the leachates is 16.2, 14.8, 1.3, 1.7 and 3.2 mg/L, respectively (Table 3). Among these constituents of health significance in drinking water, WHO (2011) proposed guideline values of 0.7 mg/L for Ba and 50 mg/L for nitrate (as NO_3^-). For Cl^-, WHO (2011) pointed out that taste (not health) thresholds for this anion are in the range of 200–300 mg/L, depending on the associated cation. Thus, Ba is the unique chemical analyzed in the leachates that exceeds the WHO (2011) constraints for drinking water. This experimental result is compatible with the high value of dissolved Ba (1.3 mg/L) found in the water sample of Grand Hotel lake (Table 1), which is certainly associated to its high levels occurring at Barreiro area.

The Enrichment Factor (EF) and Geoaccumulation Index (Igeo) have been widely used to assess the presence and intensity of anthropogenic contaminant deposition on sediments and surface soils (Barbieri, 2016). However, they require the use of a normalization procedure that offsets the variability in mineralogy and grain size that involves the choice of a conservative element (of natural origin) in the sample that exhibits a structural combination with one or more mineral phases (Guimarães et al., 2011). Another requirement is the adoption of "Geochemical Background" values, however, they have been subject of intense debates (e.g. Matschullat et al., 2000; Baize and Sterckeman, 2001; Rémy et al., 2003; Reimann and de Caritat, 2005; Galuszka, 2007).

The ratio (in $kg{\cdot}m^{-3}$) of the weight of the dissolved (radio)element per unit volume of solution to its weight per unit weight of the solid phase corresponds to a "mobility index" whose numerator and denominator tell about the liquid and solid phases, respectively (Bonotto, 1998, 2006; Bonotto and Oliveira, 2017). It is reciprocal of the following ratios (in $m^3{\cdot}kg^{-1}$): adsorption coefficient (AAEC, 1983), distribution coefficient (Richardson and McSween Jr., 1989; Krauskopf and Bird, 1995; Faure, 1998), or enrichment factor (Szalay, 1964; Langmuir, 1978).

In this paper, the equations $M_{dis} = (El)_{dis} / (El)_{sed}$ and $M_{SS} = (El)_{SS} / (El)_{sed}$ allowed calculate mobility indices (in $kg{\cdot}m^{-3}$) representing, respectively, the element presence in the liquid $[(El)_{dis}]$ and suspended solids $[(El)_{SS}]$ phases relatively to its occurrence in the solid matrix $[(El)_{sed}]$ (mean value in the sediment core). The values obtained from the data reported in Tables 1, 3 and 4 are in Table 6, indicating ranges of 10^{-6}–$118 kg/m^3$ and 2×10^{-4}–$2.2 kg/m^3$ for M_{dis} and M_{SS}, respectively. $M_{dis} > 1 kg/m^3$ in (earth) alkaline elements (Na, K, Ca, Mg) agree with their tendency of enhanced transfer into the liquid phase during weathering processes in soil profiles (Faure, 1998), whereas $M_{SS} > 1 kg/m^3$ for Na and K may suggest their preferential transport into fine feldspars particles and/or clay minerals. Chloride exhibits the highest M_{dis} value ($118 kg/m^3$), confirming its conservative behavior in solution as recognized elsewhere (e.g. Faure, 1998; Peters et al., 1992; Phillips, 2000; Mazor, 2004). Other M_{dis} and M_{SS} values in

Table 5
Matrix of the Pearson correlation coefficients involving the major oxides, minor constituents, organic matter (OM) and $^{210}Pb_T$ in the sediment core sampled at Barreiro area, Araxá city, Minas Gerais State, Brazil. The significance level (one-tailed probability value; 2 degrees of freedom) of the Pearson correlation coefficient was acceptable at 0.05. Significant correlations are in bold. nc = not calculated.

Parameter	OM	SiO_2	Al_2O_3	Fe_2O_3	TiO_2	Na_2O	K_2O	CaO	MgO	MnO	P_2O_5	BaO	Nb_2O_5	SO_3	SrO
OM	1														
SiO_2	0.17	1													
Al_2O_3	−0.03	0.53	1												
Fe_2O_3	−0.16	**−0.88**	**−0.77**	1											
TiO_2	−0.23	0.43	**0.90**	**−0.74**	1										
Na_2O	−0.61	−0.47	−0.63	0.39	−0.17	1									
K_2O	−0.25	**0.89**	0.39	−0.67	0.26	−0.39	1								
CaO	0.22	**0.82**	0.36	−0.63	0.11	−0.51	**0.94**	1							
MgO	0.10	0.46	−0.33	−0.10	−0.48	−0.16	0.38	0.53	1						
MnO	0.08	0.38	0.25	−0.19	−0.10	−0.54	0.66	**0.81**	0.34	1					
P_2O_5	0.02	**0.78**	**0.92**	**−0.89**	**0.77**	−0.53	**0.76**	**0.69**	−0.02	0.49	1				
BaO	−0.04	**−0.88**	**−0.79**	**0.83**	−0.59	0.64	**−0.93**	**−0.81**	−0.22	−0.59	**−0.94**	1			
Nb_2O_5	0.14	**−0.83**	**−0.67**	**0.75**	−0.55	0.44	**−0.95**	**−0.83**	−0.17	−0.64	**−0.88**	**0.94**	1		
SO_3	−0.02	**−0.74**	**−0.93**	**0.83**	**−0.75**	0.65	**−0.74**	−0.66	0.02	−0.50	**−0.98**	**0.95**	**0.86**	1	
SrO	−0.03	0.10	**0.82**	−0.49	**0.87**	−0.38	−0.23	−0.21	−0.65	−0.28	0.54	−0.33	−0.17	−0.56	1
ZrO_2	−0.09	0.30	**0.88**	**−0.67**	**0.97**	−0.27	0.03	−0.03	−0.56	−0.21	**0.68**	−0.47	−0.36	**−0.67**	**0.96**
Cr_2O_3	−0.16	0.26	**0.80**	−0.60	**0.93**	−0.18	−0.06	−0.16	−0.51	−0.38	0.57	−0.39	−0.26	−0.58	**0.95**
ZnO	0.09	−0.24	0.52	−0.20	0.61	0.08	−0.63	−0.52	**−0.67**	−0.52	0.17	0.07	0.27	−0.20	**0.90**
CuO	−0.04	0.32	0.63	−0.65	**0.89**	0.30	0	−0.17	−0.52	−0.56	0.49	−0.29	−0.28	−0.43	**0.78**
NiO	−0.74	0.04	**0.70**	−0.24	0.52	0.17	0.28	0.24	−0.27	0.50	0.65	−0.50	−0.49	**−0.69**	0.41
PbO	0.02	−0.58	−0.02	0.30	0.15	0.24	**−0.87**	**−0.88**	−0.55	−0.81	−0.39	0.53	0.69	0.34	0.55
ThO_2	0.04	**−0.88**	−0.65	**0.77**	−0.47	0.48	**−0.98**	**−0.90**	−0.30	**−0.70**	**−0.88**	**0.95**	**0.98**	**0.86**	−0.11
Cl	−0.54	0.58	**0.91**	**−0.89**	**0.90**	**−0.73**	0.52	0.17	−0.39	−0.02	**0.93**	**−0.80**	**−0.75**	**−0.91**	0.65
As_2O_3	0.01	0.52	−0.03	−0.18	−0.29	−0.40	**0.70**	**0.86**	**0.67**	**0.88**	0.32	−0.52	−0.62	−0.31	−0.60
Y_2O_3	−0.09	0.24	**0.90**	−0.64	**0.95**	−0.20	0.05	0.02	−0.62	−0.09	**0.71**	−0.47	−0.39	**−0.69**	**0.94**
La_2O_3	0.19	**−0.69**	−0.19	0.42	−0.10	0.24	**−0.98**	**−0.83**	−0.39	−0.68	−0.51	**0.66**	**0.85**	0.47	0.35
CeO_2	0.36	**−0.74**	−0.36	0.59	−0.42	0.07	**−0.96**	−0.65	−0.20	−0.38	−0.60	**0.68**	**0.87**	0.54	0.06
Nd_2O_3	0.03	−0.32	0.37	−0.03	0.39	0.06	**−0.77**	−0.55	−0.41	−0.48	0.03	0.14	0.40	−0.10	**0.75**
U	−0.06	0.14	**0.77**	−0.55	**0.86**	0.02	−0.24	−0.21	−0.52	−0.36	0.52	−0.29	−0.12	−0.52	**0.96**
$^{210}Pb_T$	0	**0.90**	0.31	**−0.75**	0.32	−0.21	**0.68**	0.60	0.61	0.09	0.53	**−0.67**	−0.61	−0.50	0

Parameter	ZrO_2	Cr_2O_3	ZnO	CuO	NiO	PbO	ThO_2	Cl	As_2O_3	Y_2O_3	La_2O_3	CeO_2	Nd_2O_3	U	$^{210}Pb_T$
OM															
SiO_2															
Al_2O_3															
Fe_2O_3															
TiO_2															
Na_2O															
K_2O															
CaO															
MgO															
MnO															
P_2O_5															
BaO															
Nb_2O_5															
SO_3															
SrO															
ZrO_2	1														
Cr_2O_3	**0.97**	1													

(*continued on next page*)

Table 5 (*continued*)

Parameter	ZrO_2	Cr_2O_3	ZnO	CuO	NiO	PbO	ThO_2	Cl	As_2O_3	Y_2O_3	La_2O_3	CeO_2	Nd_2O_3	U	$^{210}Pb_T$
ZnO	**0.78**	nc	1												
CuO	**0.87**	nc	nc	1											
NiO	0.46	nc	nc	nc	1										
PbO	0.35	nc	nc	nc	nc	1									
ThO_2	−0.30	−0.19	0.30	−0.16	−0.46	**0.74**	1								
Cl	**0.76**	nc	nc	nc	nc	nc	−0.65	1							
As_2O_3	−0.46	−0.56	**−0.82**	−0.64	0.20	**−0.96**	**−0.69**	−0.10	1						
Y_2O_3	**0.98**	**0.90**	**0.76**	**0.81**	0.57	0.28	−0.32	**0.74**	−0.39	1					
La_2O_3	0.14	0.22	**0.72**	0.23	−0.25	**0.92**	**0.84**	−0.40	**−0.84**	0.10	1				
CeO_2	−0.18	−0.14	0.46	−0.37	−0.29	**0.69**	**0.82**	**−0.73**	−0.55	−0.17	**0.90**	1			
Nd_2O_3	0.58	0.65	**0.91**	0.46	0.18	**0.82**	0.40	0.04	**−0.74**	0.55	**0.81**	0.62	1		
U	**0.95**	**0.96**	**0.90**	**0.83**	0.38	0.55	−0.08	0.55	−0.60	**0.92**	0.39	0.07	**0.79**	1	
$^{210}Pb_T$	0.19	0.25	−0.25	0.31	−0.14	−0.41	−0.66	0.41	0.38	0.08	−0.54	−0.66	−0.24	0.11	1

Table 6 lower than unity indicate the elements trend to remain adsorbed in the solid phase. This is highlighted by the quite low iron values, corroborating that Fe oxides and hydroxides are highly sorptive materials, exerting an important role in retaining elements in aquatic systems (e.g. Langmuir, 1978; AAEC, 1983; Rodrigues Filho and Maddock, 1997; Bonotto and Silveira, 2003). The ratio of the amount of Ba and Cl leached to the respective concentration in the sediments confirm the M_{dis} values < 1 kg/m^3 and > 1 kg/m^3, respectively, as correspond to 0.1 kg/m^3 (for Ba) and 74 kg/m^3 (for Cl). The M_{SS}/M_{dis} ratios points out that the (earth) alkaline elements Na, K, Ca, Mg, Sr, Ba and Sr prefer to remain dissolved rather than in the suspended solids phase.

4.3. Sedimentation rates and anthropogenic inputs

Bonotto and Lima (2006) investigated the grain size (< 1 mm, 0.25–0.125 mm, and < 0.062 mm) effects on the radionuclides retention in a sediment core sampled at the Corumbataí River basin, São Paulo State, Brazil (Santa Terezinha station, 16–22 cm depth). Both ^{210}Po and ^{238}U accumulated preferentially in the < 0.062 mm fraction, similarly to other trace metals that are mainly associated to finer grain size particles (Förstner and Salomons, 1980). Because the radionuclides concentration on the < 1 mm size fraction was also significant, Bonotto and Lima (2006) used the homogenized portions of the sediment core segments due to the data acquisition simplification. Despite the same approach was adopted here, the $^{210}Pb_{xs}$ mechanisms of incorporation in the finer grains would be helpful to validate several hypotheses made in the ^{210}Pb dating method, consisting on a subject that will be discussed in a different paper.

The U activity concentration, [U], as measured by alpha spectrometry was between 5.7 and 22.9 dpm/g (7.6–30.7 μg/g; average = 14.2 μg/g), yielding $^{210}Pb_s$ values of 0.9–3.7 dpm/g (Table 4). They are compatible with the U-enhanced levels at the Barreiro area, exceeding the values found in other sediment core from the region: Areia stream (0.07–1.2 μg/g; average = 0.6 μg/g), Feio stream (0.2–1.9 μg/g; average = 0.7 μg/g), Fundo stream (0.03–7.4 μg/g; average = 1.9 μg/g), and Sal stream (0.7–28.1 μg/g; average = 5.4 μg/g).

The total ^{210}Pb activity, $^{210}Pb_T$, ranged from 17.6 to 39.2 dpm/g (Table 4), decreasing according to the core depth (Fig. 5) and, therefore, favoring the application of the CF:CS ^{210}Pb chronological model. The excess ^{210}Pb activity, $^{210}Pb_{xs}$, was 15.6–37.9 dpm/g (Table 4), whilst plotting ln $^{210}Pb_{xs}$ against MD resulted in a linear ^{210}Pb profile (Fig. 6) whose slope allowed determine a sedimentation rate of 1.32 ± 0.16 gcm^{-2} yr^{-1}. Table 4 reports the deposition times and sedimentation rates calculated by the CRS model from Eqs. (1) and (2), respectively. The mean sedimentation rate of 1.49 ± 0.18 gcm^{-2} yr^{-1} differs ~11% of the value found by the CF:CS model, which is within the interval of the analytical uncertainty associated to the radiometric data.

Comparison of such sedimentation rate with some reported values in the literature either at a local or global scale indicates that the climatic conditions and hydrologic regime, among other factors, take an important role on the quite variable range of data. For instance, in Brazil, values lower than that found at the Barreiro area have been reported in Corumbataí River in São Paulo State (0.22–0.80 gcm^{-2} yr^{-1}; Bonotto and Lima, 2006), Atibaia River basin in São Paulo State (0.05–0.78 gcm^{-2} yr^{-1}; Sabaris and Bonotto, 2010), and in several Rondonian lakes (0.18–0.86 gcm^{-2} yr^{-1}; Bonotto and Vergotti, 2015). Additionally, in other countries, we have: 0.01–0.27 gcm^{-2} yr^{-1} in Canadian lakes (Turner and Delorme, 1996); 0.44–0.62 gcm^{-2} yr^{-1} in Chapala lake at Guadalajara, Mexico (Fernex et al., 2001); 0.08–0.17 gcm^{-2} yr^{-1} in Portil lagoon and Huelva estuary in southwest of Spain (San Miguel et al., 2003, 2004); 0.05–0.21 gcm^{-2} yr^{-1} in the Upper lake Radunskie, Poland (Tylmann, 2004); 0.01–0.02 gcm^{-2} yr^{-1} in lakes Puyehue and Icalma at the

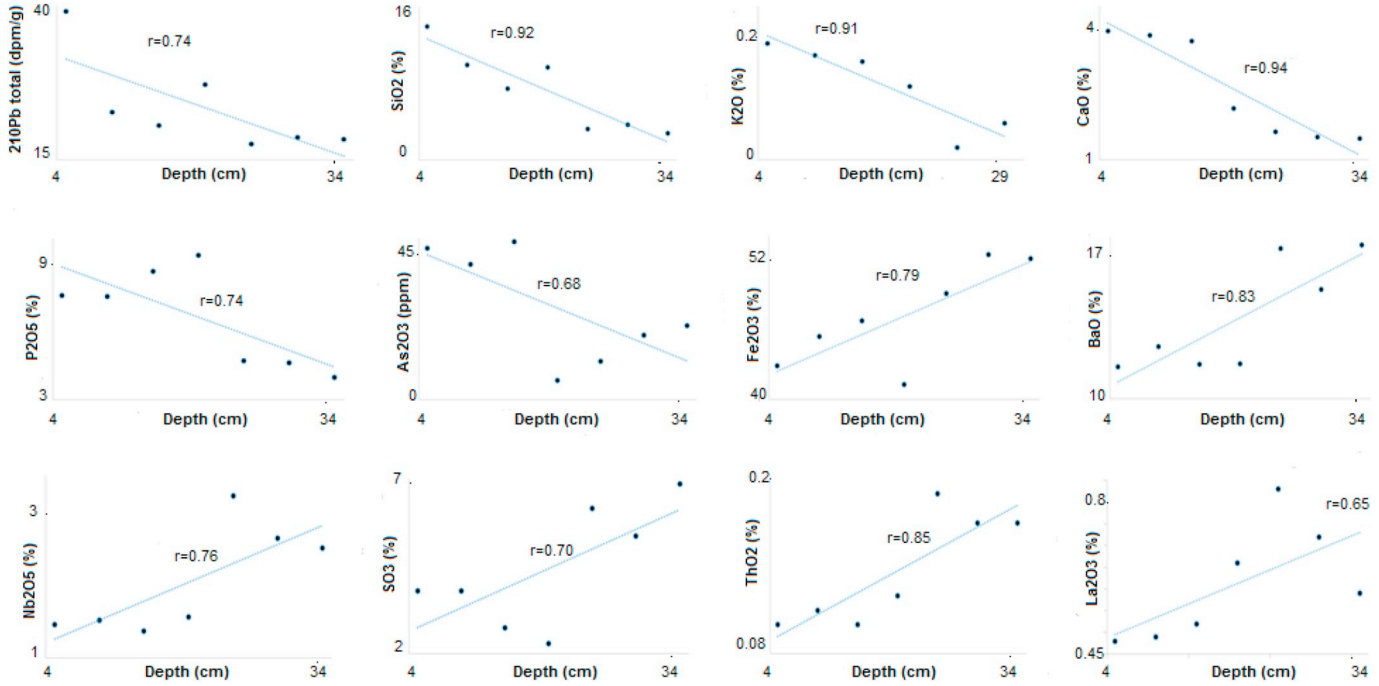

Fig. 5. Significant relationships involving several parameters analyzed and the core depth at Barreiro area, Araxá city, Minas Gerais State, Brazil.

Table 6
Mobility indices of the elements (mean value) analyzed in the sediment core and surface water of the Grand Hotel lake sampled at Barreiro area, Araxá city, Minas Gerais State, Brazil.

Element	M_{dis} [a] (kg/m^3)	M_{SS} [b] (kg/m^3)	M_{SS}/M_{dis}
Si	0.09	nc	nc
Al	0.0004	0.01	31
Fe	10^{-6}	0.0006	600
Na	23	2.2	0.1
K	5.1	1.2	0.2
Ca	1.3	0.09	0.07
Mg	13	0.09	0.007
P	0.0002	nc	nc
Ba	0.01	0.0002	0.02
S	0.1	nc	nc
Sr	0.4	0.003	0.007
Cr	0.002	0.06	32
Zn	0.0003	0.04	109
Cu	0.002	0.2	76
Ni	0.002	0.02	10
Pb	0.001	nc	nc
Cl	118	nc	nc
U	0.05	nc	nc
^{210}Po	0.01	nc	nc

nc = not calculated.
[a] $M_{dis} = (El)_{dis} / (El)_{sed}$.
[b] $M_{SS} = (El)_{SS} / (El)_{sed}$.

Chilean Lake District (Arnaud et al., 2006); 0.15–0.26 gcm^{-2} yr^{-1} in Tasek Bera lake system in southwest Pahang, Malaysia (Tahir et al., 2010). However, high rates exceeding 1 gcm^{-2} yr^{-1} as determined in the Barreiro area have been mainly reported in the tropical conditions occurring in Brazil like in the Curuaí Great Lake at Pará State (1.10–1.16 gcm^{-2} yr^{-1}; Moreira-Turcq et al., 2004), in the Amazon River mouth at Amapá State (1.09–2.51 gcm^{-2} yr^{-1}; Nery and Bonotto, 2011), or in lakes Araçá and Tucunaré at Rondônia State (1.53–1.97 gcm^{-2} yr^{-1}; Bonotto and Vergotti, 2015).

The longest deposition time obtained by the CRS and CF:CS models applied to the sediment core from the Barreiro area corresponded to 70 and 24 years, respectively (Table 4). Despite both models responded congruently to the sedimentation rates, the CRS model takes into account occasional changes on the rates of erosion and sediments accumulation at Grand Hotel lake, Barreiro area. The sampling year (2009) corresponded to the water-sediments interface at the uppermost layer. Such reference year and the use of Eq. (1) allowed determine the expected deposition year for each sediments layer. Table 4 reports the possible interval of dates for each section of the sediment core based on the statistical uncertainty of the radiometric data.

Anthropogenic inputs involving the barium release into waters occurred at Barreiro area by the early 1980s as recognized by CBMM and reported by Pinto et al. (2011). This happened because of a leakage at the tailings dam B4 (Fig. 3) as the adoption of synthetic membrane for the dam waterproofing only started in 2006 (Lemos Jr., 2012). After the environmental accident, mitigation actions took place there, which involved the efluents neutralization in the pyrochlore concentrate production unit before reaching the tailings dam B4 (Fig. 3), control and monitoring of the groundwater after barite precipitation and gradual modification of the leaching process (Pinto et al., 2011). The neutralization process adopted by CBMM consisted on the sodium sulfate addition for reacting with barium chloride and forming barite, whose solubility is low ($BaCl_2 + Na_2SO_4 \rightarrow BaSO_4 + 2\ NaCl$) (Beato et al., 2000).

Fig. 6 shows the historical trends of BaO, Nb_2O_5, SO_3, ThO_2 and REEs (La, Ce) concentrations according to the ages estimated by the CRS model. These constituents exhibit a concentration peak around the years 1971–1975. Because sediments are good archives of past contamination events, it is possible that the peaks are indicating the anthropogenic inputs in the early 1980s, which may have started before its "official" recognition, perhaps in the middle 1970s. The significant correlations among BaO, Nb_2O_5, SO_3, CeO_2, La_2O_3, and ThO_2 (Table 5 and Fig. 5) reinforce this hypothesis, suggesting they could be mobilized altogether from the tailings dam. Differently, the historical trend of Fe_2O_3 does not indicate a concentration peak around the years 1971–1975, possibly due to the strong immobile tendency of the Fe oxides and hydroxides as evidenced by the quite low M_{dis} value (10^{-6} kg/m^3, Table 6).

The validation of this dating method through an independent technique is highly recommendable, for instance, using fallout

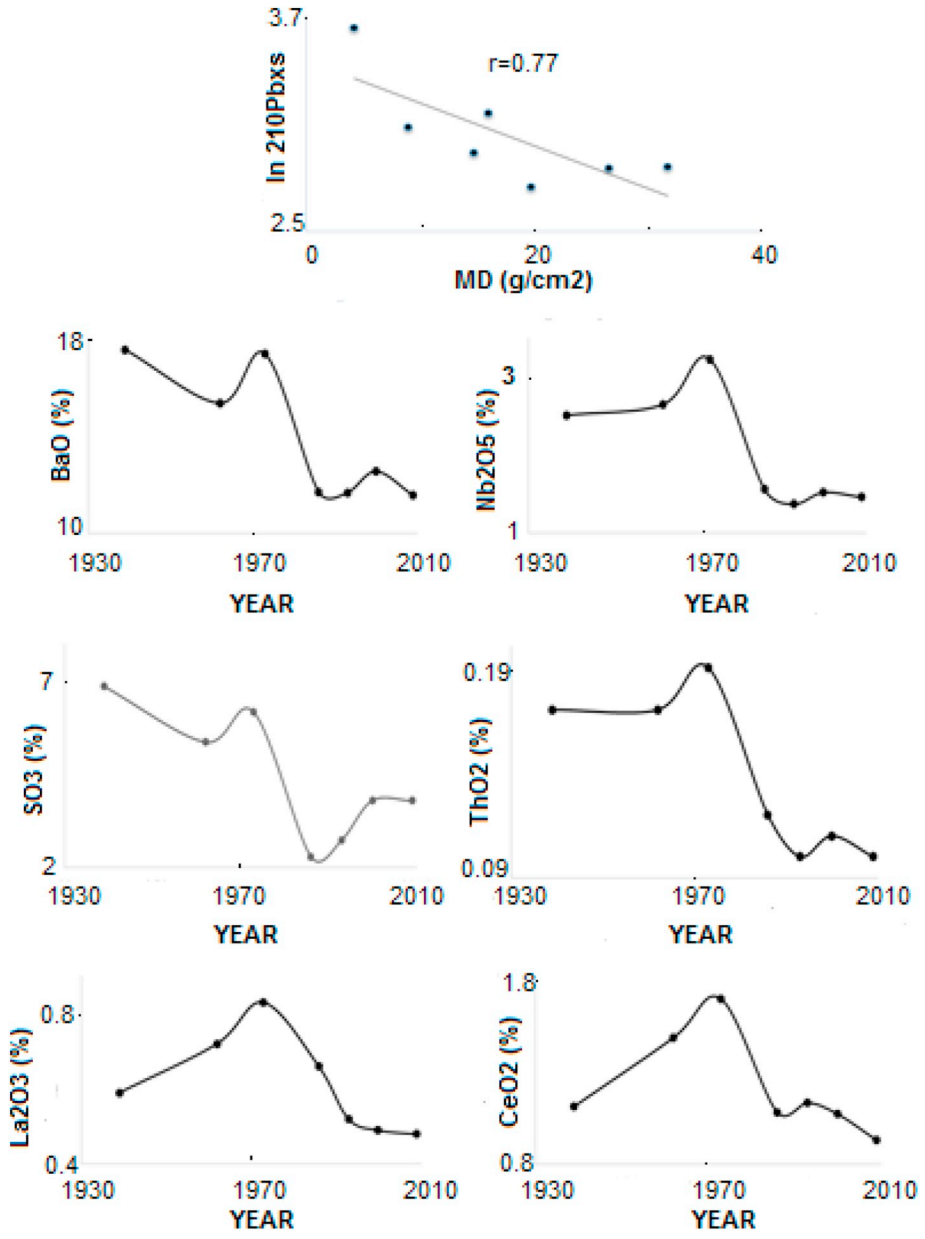

Fig. 6. Excess ^{210}Pb vs. mass depth (MD) relationship and the deposition year obtained by the CRS model plotted against the BaO, Nb_2O_5, SO_3, ThO_2 and REEs content in the sediment core sampled at Barreiro area, Araxá city, Minas Gerais State, Brazil.

radionuclides such as ^{137}Cs, ^{241}Am, ^{90}Sr or ^{239,240,241}Pu (Hong et al., 2012). However, they have been mainly released into the atmosphere of northern hemisphere and because of the fallout dependence with latitude, there is relatively scarce radionuclides fallout data in southern hemisphere. Thus, their records in sediments occurring in Brazil practically do not exist due to difficulties for finding them in detectable activities (Bonotto and Garcia-Tenorio, 2014). The expected progressive decreasing of pollutants after the adoption of synthetic membrane that started in 2006 could be checked in a future investigation considering thinner sections of the core in order to reach a better time resolution. Another helpful approache in a future paper would be an estimate (or systematic study) of how the dates obtained can be modified according to calculations that take into account other possible values of the ^{222}Rn emanation coefficient (E) from the rocks/minerals/soils/sediments. This certainly could provide diverse scenarios of that displayed here from the adoption of the extreme E value corresponding to 0.84.

5. Conclusion

Countries throughout the world have faced severe environmental problems due to mining activities, mainly those involving open-pit mines. This is also the case of Brazil that possesses a mineral potential equivalent or higher than that of other nations. This study focused the Barreiro area located at Araxá city, Minas Gerais State, in which niobium and phosphate have constituted mineral commodities largely exploited since the 60's with consequent impacts to the environment. (Radio)chemical analysis of rainwater, water and a 35-cm depth sediment core of Grand Hotel lake, leachates of the sediments sections, and groundwater of two well-known springs allowed determine barium concentrations exceeding the WHO guideline reference value of 0.7 mg/L in drinking water. The mean Cr, Zn, Cu and Pb concentration in the sediments was at least equivalent to values reported in other polluted sites elsewhere, exceeding the probable effect level (PEL) guideline established by the Canadian Council of Ministers of the

Environment (CCME) for freshwater (90, 315, 197 and 91.3 μg/g, respectively). The pronounced Ba concentration in the sediments was about 167 times higher than the guideline reference value proposed by CCME for soil use in agriculture and much above of maximum levels reached in other polluted sites. Calculated mobility indices (in $kg{\cdot}m^{-3}$) indicated tendency of enhanced transfer into the liquid phase of the (earth) alkaline elements (Na, K, Ca, Mg) and Cl that exhibited the highest value (118 kg/m^3), confirming its conservative behavior in solution. Mobility indices determined for Al, Fe, Ba, Sr, Cr, Zn, Cu and Ni in the dissolved and suspended solid phases indicated their trend to remain adsorbed in the solid phase and also pointed out the preference of the (earth) alkaline elements Na, K, Ca, Mg, Sr, Ba and Sr to remain dissolved instead in the suspend solids phase. The Constant Rate of ^{210}Pb Supply (CRS) model allowed determine an average sedimentation rate of 1.49 $g{\cdot}cm^{-2}{\cdot}yr^{-1}$ at Barreiro area that is higher than most of the values reported in other sites but equivalent to rates found under the tropical conditions occurring in Brazil. The historical trends of BaO, Nb_2O_5, SO_3, ThO_2 and REEs (La, Ce) concentrations according to the ages estimated by the CRS model showed a concentration peak around the year 1973 that could be associated with anthropogenic inputs occurring there.

Acknowledgments

The authors thank CNPq (National Council for Scientific and Technologic Development) in Brazil for financial support of this study through Grant No. 400700/2016-6 and UNESPetro for the infrastructure access. DMB thanks *Fundación Carolina*, Madrid, Spain, for the mobility scholarship at *Universidad de Sevilla*, Seville, Spain, during January and February 2018. The authors also thank two anonymous reviewers for very helpful comments that improved the readability of the manuscript.

References

AAEC (Australian Atomic Energy Commission Research Establishment), 1983. Radionuclide Migration Around Uranium Ore Bodies: Analogue of Radioactive Waste Repositories. Annual Report. AAEC, Sydney (36 pp.).

Aksil, A., Koldas, S., 2006. Acid Mine Drainage (AMD): causes, treatment and case studies. J. Clean. Prod. 14, 1139–1145. https://doi.org/10.1016/j.jclepro.2004.09.0.06.

Appleby, P.G., Oldfield, F., 1978. The calculation of ^{210}Pb dates assuming a constant rate of supply of unsupported ^{210}Pb to the sediment. Catena 5, 1–8.

Appleby, P.G., Oldfield, F., 1992. Application of lead-210 to sedimentation studies. In: Ivanovich, M., Harmon, R.S. (Eds.), Uranium Series Disequilibrium: Applications to Environmental Problems, 2nd ed. Clarendon Press, Oxford, pp. 731–778.

Argollo, R.M., 2001. Chronology of the Recent Sedimentation and Deposition of Heavy Metals at Baía de Todos os Santos Using Pb-210 and Cs-137. PhD Thesis. Federal University of Bahia, Salvador (104 pp. (in Portuguese)).

Arnaud, F., Magand, O., Chapron, E., Bertrand, S., Boës, X., Charlet, F., Mélières, M.-A., 2006. Radionuclide dating (^{210}Pb, ^{137}Cs, ^{141}Am) of recent lake sediments in a highly active geodynamic setting (Lakes Puyehue and Icalma – Chilean Lake District). Sci. Total Environ. 366, 837–850.

Baize, D., Sterckeman, T., 2001. Of the necessity of knowledge of the natural pedogeochemical background contente in the evaluation of the contamination of soils by trace elements. Sci. Total Environ. 264, 127–139.

Baran, A., Tarnawski, M., 2015. Assessment of heavy metals mobility and toxicity in contaminated sediments by sequential extraction and a battery of bioassays. Ecotoxicology 24, 1279–1293.

Barbieri, M., 2016. The importance of Enrichment Factor (EF) and Geoaccumulation Index (Igeo) to evaluate the soil contamination. J. Geol. Geophys. 5, 237. https://doi.org/10.4172/2381-8719.1000237.

Baskaran, M., Naidu, A.S., 1995. ^{210}Pb-derived chronology and the fluxes of ^{210}Pb and ^{137}Cs isotopes into continental shelf sediments, East Chukchi Sea, Alaskan Artic. Geochim. Cosmochim. Acta 59 (21), 4435–4448.

Beato, D.A.C., Viana, H.S., Davis, E.G., 2000. Evaluation and hydrogeological diagnosis of mineral waters aquifers from Barreiro, Araxá, MG, Brazil. In: ABAS (Brazilian Association of Groundwater) (Ed.), Proc. I Joint World Congress on Groundwater. ABAS, Fortaleza, pp. 1–20 (in Portuguese).

Bojakowska, I., Krasuska, J., 2014. Copper and other trace elements in sediments of lakes near Konin (Poland). J. Elem. 19 (1), 31–40.

Bonotto, D.M., 1998. Implications of groundwater weathered profile interactions to the mobilization of radionuclides. J. S. Am. Earth Sci. 11, 389–405.

Bonotto, D.M., 2006. Hydro(radio)chemical relationships in the giant Guarani aquifer, Brazil. J. Hydrol. 323, 353–386.

Bonotto, D.M., 2010. The Poços de Caldas Hot Spot: A Big Blast for Nuclear Energy in Brazil. Nova Science, New York (228 pp).

Bonotto, D.M., 2016. Hydrogeochemical study of spas groundwaters from southeast Brazil. J. Geochem. Explor. 169, 60–72.

Bonotto, D.M., Andrews, J.N., 1997. The implications of the laboratory ^{222}Rn flux measurements to the radioactivity in groundwaters: the case of a karstic limestone aquifer. Appl. Geochem. 12, 715–726.

Bonotto, D.M., Andrews, J.N., 1999. Transfer of radon and parent nuclides ^{238}U and ^{234}U from soils of Mendip Hills area, England, to the water phase. J. Geochem. Explor. 66, 255–268.

Bonotto, D.M., Caprioglio, L., 2002. Radon in groundwaters from Guarany aquifer, South America: environmental and exploration implications. Appl. Radiat. Isot. 57 (6), 931–940.

Bonotto, D.M., Garcia-Tenorio, R., 2014. A comparative evaluation of the CF:CS and CRS models in ^{210}Pb chronological studies applied to hydrographic basins in Brazil. Appl. Radiat. Isot. 92, 58–72.

Bonotto, D.M., Lima, J.L.N., 2006. ^{210}Pb-derived chronology in sediment cores evidencing the anthropogenic occupation history at Corumbataí River basin, Brazil. Environ. Geol. 50 (4), 595–611.

Bonotto, D.M., Oliveira, A.M.M.A., 2017. Mobility indices and doses from ^{210}Po and ^{210}Pb activity concentrations data in Brazilian spas groundwaters. J. Environ. Radioact. 172, 15–23.

Bonotto, D.M., Silveira, E.G., 2003. Preference ratios for mercury and other chemical elements in the Madeira river, Brazil. J. S. Am. Earth Sci. 15, 911–923.

Bonotto, D.M., Vergotti, M., 2015. ^{210}Pb and compositional data of sediments from Rondonian lakes, Madeira River basin, Brazil. Appl. Radiat. Isot. 99, 5–19.

Bonotto, D.M., Caprioglio, L., Bueno, T.O., Lazarindo, J.R., 2009. Dissolved ^{210}Po and ^{210}Pb in Guarani aquifer groundwater, Brazil. Radiat. Meas. 44, 311–324.

Braga, J.R.K., Born, H., 1988. Geological and mineralogical characteristics of the apatite mineralization at Araxá. In: SBG (Brazilian Society of Geology) (Ed.), Proc. XXXV Brazilian Congress of Geology. v. 1. SBG, Belém, pp. 219–226 (in Portuguese).

Brownlow, A.H., 1996. Geochemistry, 2nd ed. Prentice-Hall, Englewood Cliffs (580 pp).

Castro, L.O., Souza, J.M., 1970. Study of Uranium and Rare Earths Associated to Niobium at Araxá – MG. IPR (Radioactive Researches Institute), Belo Horizonte (59 pp. (in Portuguese)).

CBMM (Brazilian Company of Mining and Metallurgy), 2015. Rare earths stockpiles. In: CETEM (Center of Mineral Technology) (Ed.), Proc. III Brazilian Seminar of Rare Earths. CETEM, Rio de Janeiro, pp. 1–27. www.cetem.gov.br/images/palestras/2015/iiisbtr/04-tadeu-carneiro.pdf>, Accessed date: 25 January 2018 (in Portuguese).

CCME (Canadian Council of Ministers of the Environment), 1995. Protocol for the Derivation of Canadian Sediment Quality Guidelines for the Protection of Aquatic Life. Environment Canada, Ottawa, pp. 1–35.

CCME (Canadian Council of Ministers of the Environment), 2001. Canadian Sediment Quality Guidelines for the Protection of Aquatic Life: Summary Tables. Environment Canada, Ottawa, pp. 1–5.

CCME (Canadian Council of Ministers of the Environment), 2013. Canadian Soil Quality Guidelines for Barium: Protection of Human Health – Scientific Criteria Document. CCME, Winnipeg (74 pp).

Chang, J.-S., Yu, K.-C., Tsai, L.-J., Ho, S.-T., 1998. Spatial distribution of heavy metals in bottom sediment of Yenshui River, Taiwan. Water Sci. Technol. 38 (11), 159–167.

Cresswell, R.G., Bonotto, D.M., 2008. Some possible evolutionary scenarios suggested by ^{36}Cl measurements in Guarani aquifer groundwaters. Appl. Radiat. Isot. 66, 1160–1174.

CSWRCB (California State Water Resources Control Board), 1995. Compilation of Sediment & Soil Standards, Criteria & Guidelines. Quality Assurance Technical Document 7. CSWRCB, Sacramento, California, pp. 1–70.

DA (Araxá Daily), 2008. Dwellers residents process mining companies and ask for a compensation of R$ 16.3 million. http://www.diariodearaxa.com.br/index.php?go=noticia&ed=20&id=1091, Accessed date: 21 September 2010 (in Portuguese).

DA (Araxá Daily), 2009. CBMM presents a defense to the action brought by the Barreiro residents. http://www.diariodearaxa.com.br/index.php?go=noticia&ed=20&id=1652, Accessed date: 21 September 2010 (in Portuguese).

DiBello, P.M., Manganaro, J.L., Aguinaldo, E.R., 1991. Barium compounds. In: Kirk-Othmer Encyclopedia of Chemical Technology, 4th ed. v. 3. John Wiley and Sons, New York, pp. 909–931.

do Rio, M.A.P., 1999. Non-Nuclear Mining Industries and Increase to the Natural Radiation Exposure. PhD Thesis. UFRJ (Federal University of Rio de Janeiro), Rio de Janeiro (130 pp. (in Portuguese)).

El-Daoushy, F., 1988. A summary on the lead-210 cycle in nature and related applications in Scandinavia. Environ. Int. 14, 305–319.

Faure, G., 1998. Principles and Applications of Geochemistry, 2nd ed. Prentice-Hall, Upper Saddle River, NJ (600 pp).

Fernex, F., Valle, P.Z., Sanchez, H.R., Michaud, F., Parron, P., Dalmasso, J., Funel, G.B., Arroyo, M.G., 2001. Sedimentation rates in Lake Chapala (Western Mexico): possible active tectonic control. Chem. Geol. 177, 213–228.

Filipek, L.H., Nordstrom, D.K., Ficklin, W.H., 1987. Interaction of acid mine drainage with waters and sediments of West Squaw Creek in the West Shasta mining district, California. Environ. Sci. Technol. 21, 388–396.

Fontana, L., Albuquerque, A.L.S., Brenner, M., Bonotto, D.M., Sabaris, T.P.P., Pires, M.A.F., Cotrim, M.E.B., Bicudo, D.C., 2014. The eutrophication history of a tropical water supply reservoir in Brazil. J. Paleolimnol. 51, 29–43.

Förstner, U., Salomons, W., 1980. Trace metal analysis on polluted sediments-I: assessment of sources and intensities. Environ. Sci. Technol. Lett. 1, 494–505.

FUNTEC (Minas Gerais Technological Center Foundation), 1984. Ecological Conflict Diagnosis Report Including Recommended Works and Measures for Mitigation of the Ecological Impact Due to Mining, Vols. 1 and 2. Technical Report. ECOS–Geology,

Consulting and Services Ltd., Araxá (in Portuguese).
Galuszka, A., 2007. Different approaches in using and understanding the term "Geochemical Background" – practical implications for environmental studies. Pol. J. Environ. Stud. 16 (3), 389–395.
Gibson, S.A., Thompson, R.N., Leonardos, O.K., Dickin, A.P., Mitchell, J.G., 1995. The Late Cretaceous impact of the Trindade mantle plume - evidence from large-volume, mafic, potassic magmatism in SE Brazil. J. Petrol. 36, 189–229.
Gomes, R.C., 2006. Technological Characterization and Systems of Mining Wastes Disposal. Technical Report. NUGEO/UFOP (Geotechnical Center of the School of Mines/Federal University of Ouro Preto), Ouro Preto (210 pp. (in Portuguese)).
Gomes, C.B., Comin-Chiaramonti, P., 2005. Some notes on the Alto Paranaíba Igneous Province. In: Comin-Chiaramonti, P., Gomes, C.B. (Eds.), Mesozoic to Cenozoic Alkaline Magmatism in the Brazilian Platform. EDUSP, São Paulo, pp. 317–340 (in Portuguese).
Gray, N.F., 1996. Field assessment of acid mine drainage contamination in surface and ground water. Environ. Geol. 27, 358–361. https://doi.org/10.1007/BF00766705.
Guimarães, G.M., Franklin, R.L., Figueiredo, A.M.G., Silva, P.S.C., Fávaro, D.I.T., 2011. Enrichment Factor and Geoaccumulation Index applied to sediment samples from Guarapiranga reservoir, Brazil, for metal and trace elements assessment. In: ABEN (Brazilian Association of Nuclear Energy) (Ed.), Proc. International Nuclear Atlantic Conference – INAC. ABEN, Belo Horizonte, pp. 1–13.
Hach, 1992. Water Analysis Handbook, 2nd ed. Hach Co., Loveland (831 pp).
Hillman, A.L., Abbott, M.B., Valero-Garcés, B.L., Morellon, M., Barreiro-Lostres, F., Bain, D.J., 2017. Lead pollution resulting from Roman gold extraction in northwestern Spain. The Holocene 27 (10), 1465–1474.
Hong, G.H., Hamilton, T.F., Baskaran, M., Kenna, T.C., 2012. Applications of anthropogenic radionuclides as tracers to investigate marine environmental processes. In: Baskaran, M. (Ed.), Handbook of Environmental Isotope Geochemistry. Springer, Berlin, pp. 367–394.
Huong, N.T.L., Ohtsubo, M., Li, L., Higashi, T., Kanayama, M., 2010. Heavy metal characterization and leachability of organic matter-rich river sediments in Hanoi, Vietnam. Int. J. Soil Sediment Water 3 (1) (article 5). http://scholarworks.umass.edu/intljssw/vol3/iss1/5, Accessed date: 25 January 2018.
Issa Filho, A., Lima, P.R.A.S., Souza, O.M., 1984. Geological aspects of Barreiro carbonatite complex, Araxá, MG, Brasil. In: Rodrigues, C.S., Lima, P.R.A.S. (Eds.), Carbonatite Complexes in Brazil: Geology. CBMM, São Paulo, pp. 20–44 (in Portuguese).
Karbassi, A.R., Nabi-Bidhendi, G.R., Bayati, I., 2005. Environmental Geochemistry of Heavy Metals in a sediment core off Bushehr, Persian Gulf. Iran. J. Environ. Health Sci. Eng. 2 (4), 255–260.
Komárek, M., Zeman, J., 2004. Dynamics of Cu, Zn, Cd, and Hg release from sediments at surface conditions. Bull. Geosci. 79 (2), 99–106.
Kotarba, A., Lokas, E., Wachniew, P., 2002. ^{210}Pb dating of young Holocene sediments in high-mountains lakes of the Tatra mountains. Geochronometria 21, 73–78.
Krauskopf, K.B., Bird, D.K., 1995. Introduction to Geochemistry. McGraw-Hill Inc., New York (647 pp).
Krishnaswami, S., Lal, D., Martin, J.M., Meybeck, M., 1971. Geochronology of lake sediments. Earth Planet. Sci. Lett. 11, 407–414.
Krupp, K., Baskaran, M., Brownlee, S.J., 2017. Radon emanation coefficients of several minerals: how they vary with physical and mineralogical properties. Am. Mineral. 102, 1375–1383.
Langmuir, D., 1978. Uranium solution-mineral equilibria at low temperatures with applications to sedimentary ore deposits. Importance in the geochemical enrichment of UO_2^{2+} and other cations. Geochim. Cosmochim. Acta 42, 547–569.
Lemos Jr., M.A., 2012. Studies for Evaluating the Capacity of the Niobium Wastes Reservoir. Ms Dissertation. School of Mines/Federal University of Ouro Preto, Ouro Preto (118 pp. (in Portuguese)).
Long, E.R., MacDonald, D.D., Smith, S.L., Calder, F.D., 1995. Incidence of adverse biological effects within ranges of chemical concentrations in marine and estuarine sediments. Environ. Manag. 19 (1), 81–97.
MacDonald, D.D., 1993. Development of an Approach to the Assessment of Sediment Quality in Florida Coastal Waters. MacDonald Environmental Services, Ltd., Ladysmith, BC (133 pp).
Matamet, F.R.M., Bonotto, D.M., 2013. Evaluation of the chromium contamination at Ribeirão dos Bagres, Franca (SP), Brazil, by the ^{210}Pb method. Appl. Radiat. Isot. 82, 359–369.
Matamet, F.R.M., Bonotto, D.M., 2018. A ^{210}Pb chronological study in sediments from Poços de Caldas Alkaline Massif (PCAM), Brazil. Appl. Radiat. Isot. 137, 108–117.
Matschullat, J., Ottenstein, N.R., Reimann, C., 2000. Geochemical background – can we calculate it? Environ. Geol. 39, 990–1000.
Maurice-Bourgoin, L., Aalto, R., Rheault, L., Guyot, J.L., 2003. Use of ^{210}Pb geochronology to explore the century-scale mercury contamination history and the importance of floodplain accumulation in Andean tributaries of the Amazon River. In: CBPM (Bahia State Company of Mineral Research) (Ed.), Short Papers of the IV South American Symposium on Isotope Geology. CBPM, Salvador, pp. 449–452.
Mazor, E., 2004. Chemical and Isotopic Groundwater Hydrology, 3rd ed. Marcel Dekker, Inc., New York (453 pp).
Melfi, A.J., Misi, A., Campos, D.A., Cordani, U.G., 2016. Mineral Resources in Brazil: Problems and Challenges. Brazilian Academy of Sciences, Rio de Janeiro (420 pp. (in Portuguese)).
Moreira-Turcq, P.M., Jouanneau, J.M., Turck, B., Seyler, P., Weber, O., Guyot, J.L., 2004. Carbon sedimentation at Lago Grande de Curuai, a floodplain lake in the low Amazon region: insights into sedimentation rates. Palaeogeogr. Palaeoclimatol. Palaeoecol. 214 (1–2), 27–40.
Munsell, 1975. Soil Color Charts. Macbeth, Baltimore.
Nery, J.R., Bonotto, D.M., 2011. ^{210}Pb and composition data of near-surface sediments and interstitial waters evidencing anthropogenic inputs in Amazon River mouth, Macapá, Brazil. J. Environ. Radioact. 102, 348–362.
Nimer, E., 1972. Test of a new method of climate classification: contribution to intertropical and subtropical climatology, especially from Brazil. Boletim de Geografia 31 (277), 141–153 (in Portuguese).
Nurlidia, M., 2008. Investigation of Lead and Zinc Dispersion From an Abandoned Mine Site at Tyndrum, Scotland (PhD Thesis). University of Glasgow, Glasgow.
Peters, C.A., Striegl, R.G., Mills, P.C., Healy, R.W., 1992. Effects of low-level radioactive-waste disposal on water chemistry in the unsaturated zone at a site near Sheffield, Illinois, 1982–1984. In: U.S. Geological Survey Water-Supply Paper 2390. U.S. Geological Survey, Denver (73 pp).
Phillips, F.M., 2000. Cholorine-36. In: Cook, P.G., Herczeg, A.L. (Eds.), Environmental Tracers in Subsurface Hydrology. Kluwer Academic, Dordrecht, pp. 299–348.
Pinto, C.L.L., Dutra, J.I.G., Salum, M.J.G., Ganine, J.F., Oliveira, M.S., 2011. Study case: major center producing phosphate and niobium in the country. In: Fernandes, F.R.C., Enriquez, M.A., Alamino, R.C.J. (Eds.), Mineral Resources & Territorial Sustainability. vol. v. 1. CETEM/MCTI, Rio de Janeiro, pp. 283–305 (in Portuguese).
Piper, A.M., 1944. A graphic procedure in the geochemical interpretation of water analyses. Trans. Am. Geophys. Union 25, 914–928.
RBM (Brasil Mineral Magazine), 2012. Ores exploration at Araxá (MG) and Tapira (MG) affect the environment. http://verbetes.cetem.gov.br/verbetes/ExibeVerbete.aspx?verid=114, Accessed date: 15 January 2018 (in Portuguese).
Reimann, C., de Caritat, P., 2005. Distinguishing between natural and anthropogenic sources of element in the environment: regional geochemical surveys versus enrichment factors. Sci. Total Environ. 337, 91–107.
Rémy, S., Prudent, P., Hissler, C., Probst, J.L., Krempp, G., 2003. Total mercury concentrations in an industrialized catchment, the Thur River Basin (north-eastern France): geochemical background level and contamination factors. Chemosphere 52, 635–644.
Rice, E.W., Baird, R.B., Eaton, A.D., Clesceri, L.S., 2012. Standard Methods for the Examination of Water and Wastewater, 22nd ed. American Public Health Association/American Water Works Association/Water Environment Federation, Washington, DC (1496 pp).
Richardson, S.M., McSween Jr., H.Y., 1989. Geochemistry: Pathways and Processes. Prentice-Hall Inc., New Jersey (487 pp).
Robbins, J.A., 1978. Geochemical and geophysical applications of radioactive lead isotopes. In: Nriagu, J.O. (Ed.), Biochemistry of Lead. Elsevier, Amsterdam, pp. 285–393.
Rodrigues Filho, S., Maddock, J.E.L., 1997. Mercury pollution in two gold mining areas of the Brazilian Amazon. J. Geochem. Explor. 58, 231–240.
Roveratti, G., Bonotto, D.M., 2017. Optimization of an x-rays fluorescence spectrometer for analyzing a tantalite sample. In: Veress, B., Szigethy, J. (Eds.), Horizons in Earth Science Research. Nova Science, New York, pp. 225–240.
Saad, A.F., Abdallah, R.M., Hussein, N.A., 2018. Physical and geometrical parameters controlling measurements of radon emanation and exhalation from soil. Appl. Radiat. Isot. 137, 273–279.
Sabaris, T.P.P., Bonotto, D.M., 2010. Sedimentation rates in Atibaia River basin, São Paulo State, Brazil, using ^{210}Pb as geochronometer. Appl. Radiat. Isot. 69, 275–288.
San Miguel, E.G., Bolívar, J.P., García-Tenorio, R., Martín, J.E., 2001. ^{230}Th/^{232}Th activity ratios as a chronological marker complementing ^{210}Pb dating in an estuarine system affected by industrial releases. Environ. Pollut. 112, 361–368.
San Miguel, E.G., Bolívar, J.P., García-Tenorio, R., 2003. Mixing, sediment accumulation and focusing using ^{210}Pb and ^{137}Cs. J. Paleolimnol. 29, 1–11.
San Miguel, E.G., Bolívar, J.P., García-Tenorio, R., 2004. Vertical distribution of Th-isotope ratios, ^{210}Pb, ^{226}Ra, and ^{137}Cs in sediment cores from an estuary affected by anthropogenic releases. Sci. Total Environ. 318, 143–157.
Santos, M.S., Carneiro, L.G., Medeiros, G., Sampaio, C., Martorell, A.B.T., Gouvea, S., Cunha, K.M.D., 2011. PIXE analyses applied to characterize water samples. In: ABEN (Brazilian Association of Nuclear Energy) (Ed.), Proc. International Nuclear Atlantic Conference – INAC. ABEN, Belo Horizonte, pp. 1–6.
Schoeller, H., 1962. Groundwaters. Masson & Cie, Paris (642 pp. (in French)).
Shang, Z., Ren, J., Tao, L., Wang, X., 2015. Assessment of heavy metals in surface sediments from Gansu section of Yellow River, China. Environ. Monit. Assess. 187 (3), 79. https://doi.org/10.1007/s10661-015-4328-6.
Shepard, F.P., 1954. Nomenclature based on sand-silt-clay ratios. J. Sediment. Petrol. 24, 151–158.
Simpson, S.L., Batley, G.E., Chariton, A.A., Stauber, J.L., King, C.K., Chapman, J.C., Hyne, R.V., Gale, S.A., Roach, A.C., Maher, W.A., 2005. Handbook for Sediment Quality Assessment. CSIRO, Bangor, NSW (117 pp).
Stoffers, P., Summerhayes, C., Forstner, U., Patchineelam, S.R., 1977. Copper and other heavy metal contamination in sediments from New Bedford Harbor, Massachusetts: a preliminary note. Environ. Sci. Technol. 11 (8), 619–621.
Szalay, A., 1964. Cation exchange properties of humic acids and their importance in the geochemical enrichment of UO_2^{2+} and other cations. Geochim. Cosmochim. Acta 28, 1605–1614.
Tahir, W.Z.W.M., Gharibreza, M.R., Latif, J.A., Yusof, J.M., Mamat, K., 2010. A preliminary study on sedimentation rate in Tasek Bera estimated using ^{210}Pb dating technique. IAEA, Vienna, pp. 1–9. https://inis.iaea.org/collection/NCLCollectionStore/_Public/43/035/43035295.pdf, Accessed date: 15 August 2018.
Tessier, A., Campbell, P.G.C., Bisson, M., 1979. Sequential extraction procedure for the speciation of particulate trace metals. Anal. Chem. 51 (7), 844–851.
Traversa, G., Gomes, C.B., Brotzu, P., Buraglini, N., Morbidelli, L., Principato, M.S., Ronca, S., Ruberti, E., 2001. Petrography and mineral chemistry of carbonatites and mica-rich rocks from the Araxá complex (Alto Paranaíba Province, Brazil). An. Acad. Bras. Cienc. 73, 71–98.
Turner, L.J., Delorme, L.D., 1996. Assessment of ^{210}Pb data from Canadian lakes using the

CIC and CRS models. Environ. Geol. 28 (2), 78–87.
Tylmann, W., 2004. Estimating recent sedimentation rates using ^{210}Pb on the example of morphologically complex lake (Upper lake Radunskie, N Poland). Geochronometria 23, 21–26.
U.S. EPA (United States Environmental Protection Agency), 1994. Acid Mine Drainage Prediction. Technical Document. U.S. EPA, Washington, DC, pp. 1–48. http://water.epa.gov/polwaste/nps/upload/amd.pdf, Accessed date: 30 January 2018.
U.S. FWS (United States Fish & Wildlife Service), 2007. Sediment quality within the impounded reaches of Cape Fear River locks and dams. http://www.fws.gov/nc-es/ecotox/reports.html, Accessed date: 1 February 2018.
U.S. NOAA (United States National Oceanic and Atmospheric Division), 1999. Sediment Quality Guidelines Developed for the National Status and Trends Program. National Ocean Service, Silver Spring, MD, pp. 1–12.
Udden, J.A., 1898. Mechanical Composition of Wind Deposits. 1. Augustana Library Publ., pp. 1–69.
UNSCEAR (United Nations Scientific Committee on the Effects of Atomic Radiation), 2000. Sources and effects of ionizing radiation. In: Report to the General Assembly, With Scientific Annexes. United Nations, New York.
USGS (United States Geological Survey), 2018. Mineral resources on-line spatial data: Araxá. https://mrdata.usgs.gov/mrds/show-mrds.php?dep_id=10068132, Accessed date: 29 January 2018.
van de Wiel, H.J., 2003. Determination of Elements by ICP-AES and ICP-MS. National Institute of Public Health and the Environment (RIVM), Bilthoven, The Netherlands (37 pp).
Viana, H.S., Davis, E.G., Beato, D.A.C., Cabral, J.A.L., 1999. Araxá Project: Geoenvironmental Study of Mineral Springs. CPRM (Brazilian Geological Survey), Belo Horizonte (125 pp. (in Portuguese)).
Vieira, J.L., 2004. The Mining Code and Additional Legislation, 2nd ed. Edipro, São Paulo (208 pp. (in Portuguese)).
Wanty, R.B., Lawrence, E.P., Gundersen, L.C.S., 1992. A theoretical model for the flux of radon from rock to groundwater. In: Gates, A.E., Gundersen, L.C.S. (Eds.), Geologic Controls on Radon. Geol. Soc. of America Spec. Paper 271, Boulder, pp. 73–78.
Wentworth, C.K., 1922. A scale of grade and class terms for clastic sediments. J. Geol. 30 (5), 377–392.
WHO (World Health Organization), 2011. Guidelines for Drinking Water Quality, 4th ed. WHO Press, Geneva (541 pp).
Widerlund, A., Roos, P., Gunneriusson, L., Ingri, J., Holmström, H., 2002. Early diagenesis and isotopic composition of lead in Lake Laisan, northern Sweden. Chem. Geol. 187, 183–197.
Widerlund, A., Chlot, S., Öhlander, B., 2014. Sedimentary records of δ^{13}C, δ^{15}N and organic matter accumulation in lakes receiving nutrient-rich mine waters. Sci. Total Environ. 485–486, 205–215.
Yao, S., Xue, B., 2016. Sediment records of the metal pollution at Chihu Lake near a copper mine at the Middle Yangtze River in China. J. Limnol. 75 (1), 2008–2016.
Young, H.D., 1962. Statistical Treatment of Experimental Data. McGraw Hill, New York (172 pp).